Open Peer Review Journal

The physics of the Earth's atmosphere I. Phase change associated with tropopause.

Michael Connolly [1]**, *Ronan Connolly*** [*1]

[1] *Connolly Scientific Research Group. Dublin, Ireland.*

Abstract

Atmospheric profiles in North America during the period 2010-2011, obtained from archived weather balloon radiosonde measurements, were analysed in terms of changes of molar density (D) with pressure (P). This revealed a pronounced phase change at the tropopause. The air above the troposphere (i.e., in the tropopause/stratosphere) adopted a "heavy phase", distinct from the conventional "light phase" found in the troposphere. This heavy phase was also found in the lower troposphere for cold, Arctic winter radiosondes.

Reasonable fits for the complete barometric temperature profiles of all of the considered radiosondes could be obtained by just accounting for these phase changes and for changes in humidity. This suggests that the well-known changes in temperature lapse rates associated with the tropopause/stratosphere regions are related to the phase change, and not "ozone heating", which had been the previous explanation.

Possible correlations between solar ultraviolet variability and climate change have previously been explained in terms of changes in ozone heating influencing stratospheric weather. These explanations may have to be revisited, but the correlations might still be valid, e.g., if it transpires that solar variability influences the formation of the heavy phase, or if the changes in incoming ultraviolet radiation are redistributed throughout the atmosphere, after absorption in the stratosphere.

The fits for the barometric temperature profiles did not require any consideration of the composition of atmospheric trace gases, such as carbon dioxide, ozone or methane. This contradicts the predictions of current atmospheric models, which assume the temperature profiles are strongly influenced by greenhouse gas concentrations. This suggests that the greenhouse effect plays a much smaller role in barometric temperature profiles than previously assumed.

Citation:
M. Connolly, and R. Connolly (2014). *The physics of the Earth's atmosphere I. Phase change associated with tropopause.*, Open Peer Rev. J., 19 (*Atm. Sci.*), ver. 0.1 (non peer reviewed draft).
URL: http://oprj.net/articles/atmospheric-science/19

Version: 0.1 (non peer-reviewed)
First submitted: January 8, 2014.
This version submitted: February 7, 2014.
This work is licensed under a Creative Commons Attribution-ShareAlike 4.0 International License.

1 Introduction

In this paper (Paper I), together with two companion papers (henceforth, Paper II[2] and Paper III[3]), we develop a new approach for describing and explaining the temperature and energy profiles of the atmosphere. This approach highlights a number of flaws in the conventional approaches, and appears to yield simpler and more accurate predictions.

In the current paper (Paper I), we will analyse weather balloon data taken from public archives, in terms of changes of molar density with pressure, and related variables. By doing so, we discover a phase change associated with the troposphere-tropopause transition, which also occurs in the lower troposphere under cold, polar winter conditions. We find that when this phase change is considered, the changes in temperature with atmospheric pressure (the *barometric temperature profiles*) can be described in relatively simple terms. These descriptions do not match the radiative physics-based infra-red cooling/radiative heating explanations used by current models. We present theoretical explanations of these simple descriptions from thermodynamic principles.

*Corresponding author: ronanconnolly@yahoo.ie. Website: http://globalwarmingsolved.com

In Paper II[2], we will argue that this previously overlooked phase change is due to partial multimerization of the main atmospheric gases, and therefore is a phase change which has not been considered by the current climate models. If this theory is correct, then this offers new insight into the formation of jet streams, tropical cyclones, polar vortices, and more generally, cyclonic and anti-cyclonic conditions. It also offers a new mechanism for the formation of ozone in the ozone layer, and a mechanism for radiative loss from the atmosphere which has been neglected until now.

In Paper III[3], we identify a mechanism for mechanical energy transmission that is not considered by current atmospheric models, which we call *"pervection"*. We carry out laboratory experiments which reveal that pervection can be several orders of magnitude faster than the three conventional heat transmission mechanisms of conduction, convection and radiation. This could be fast enough to keep the atmosphere in thermodynamic equilibrium over the distances from the troposphere to the stratosphere, thereby contradicting the conventional assumption that the lower atmosphere is only in *local* thermodynamic equilibrium.

The format of the current paper is as follows. In Section 2 we will briefly review the conventional descriptions and explanations for the atmospheric temperature and energy profiles. In Section 3 we present our analysis of the atmospheric temperature profiles in terms of molar density. In Section 4, we will consider the implications of our findings. Finally, in Section 5, we offer some concluding remarks.

2 Conventional explanations for the atmospheric temperature and energy profiles

2.1 The atmospheric "layers"

Traditionally the atmosphere has been schematically divided into a number of layers or "spheres" surrounding the earth. The schematic divisions are allocated on the basis of the temperature profiles in each region.

The three lowest spheres (the "troposphere", "tropopause" and "stratosphere") contain more than 99% of the atmosphere by mass. Since, the weather balloons which we analyse in this paper only reach the stratosphere before bursting, our discussion will be mostly confined to these three lower layers.

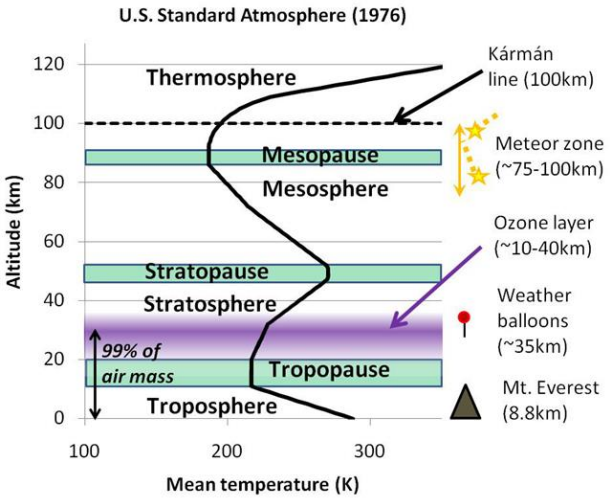

Figure 1: *Variation of temperature with altitude, as estimated by the U.S. Standard Atmosphere, 1976[1] (*thick solid black line*). Altitude represents height above sea level. The Kármán line (*dashed black line*) of 100 km is an arbitrary value often chosen to represent the "boundary" between the atmosphere and "space".*

The name *troposphere* is derived from the Greek word "*tropos*", meaning to mix or stir. According to the US Standard Atmosphere[1] (Figure 1), for every kilometre travelled upwards from the ground through the troposphere, the temperature drops by about 6.5K. This is due to thermal energy being converted into gravitational potential energy. The troposphere varies in thickness from about 15 km at the Equator to half that thickness at the Poles (see Figure 2). The lowest one or two kilometres of the troposphere (where most rain and clouds occur) is sometimes called the *"boundary layer"*.

In the *tropopause* the temperature does not change with height, hence the suffix "*–pause*". The thickness of the tropopause also changes from the Equator to the Poles, but in the opposite direction to that of the troposphere, i.e. it is thickest at the Poles and thinnest at the Equator (see Figure 2).

In the *stratosphere* the temperature increases with height. It is often assumed that hot air is always less dense than cold air. This assumption leads to the incorrect conclusion that warm air has to float above cold air. For this reason, mixing of air between different layers is assumed to be rare, leading to the

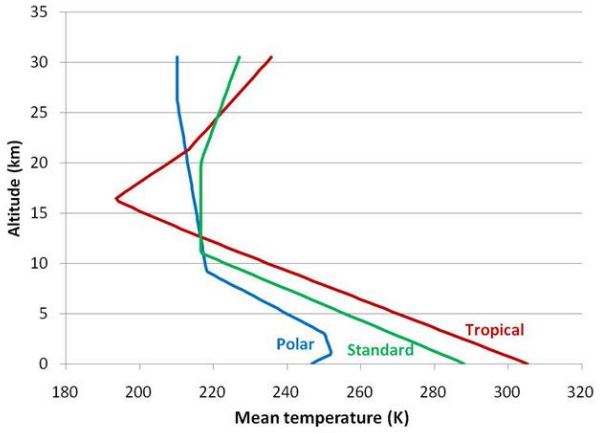

Figure 2: *Polar, standard mid-latitude and tropical altitudinal temperature profiles. Data taken from the US Defense Department's "Non-standard atmospheres" dataset, downloaded from the Public Domain Aeronautical Software website (original source: document MIL-STD-210A). Temperatures were converted from degrees Rankine, and altitudes from feet.*

belief that the air in the region is essentially stratified (hence the prefix "*strato–*"). Some researchers have disputed this assumption, e.g., Brewer, 1949[4], but the name has stuck. As a consequence, there is a general perception that the stratosphere is mostly isolated from the troposphere, except for some complex circulation patterns confined to specific areas, e.g., the tropical tropopause layer[5, 6] or the Brewer-Dobson circulation in the Arctic[7, 8].

2.2 Assumptions used for the conventional explanations

The current theories to explain these temperature profiles are based on radiative convective models - see Edwards, 2011 for a review of their historical development[9]. These models are based on a number of assumptions about the physics of the atmosphere:

1. Conduction is assumed to be a negligible mechanism for energy transmission in the atmosphere. This is a reasonable assumption, since air is known to be a relatively poor conductor.

2. Vertical convection is assumed to be well-explained by the *"Rising Air Column"* theory initially developed in the 17th and 18th centuries by Halley, Hadley, Ferrell, et al.[9]. This is based on the idea that "hot air rises" mentioned above.

3. Horizontal convection is assumed to be well-explained by Bjerknes' so-called *"primitive equations"*, i.e., Newton's laws, the Navier-Stokes relationships and mass conservation[9].

4. Convection is believed to be a significant energy transmission mechanism in the troposphere, but less significant in the tropopause/stratosphere. This is because of the assumption that "hot air rises", and that air in the stratosphere is therefore "stratified".

5. It is typically assumed that the mean atmospheric temperature profiles are strongly influenced by radiative transfer mechanisms[10, 11]. For this reason, energy transmission in current atmospheric models is heavily dominated by radiative processes, e.g., Refs. [12–14].

6. Phase changes also offer another mechanism for energy transfer. It is generally agreed that an additional heat transfer mechanism with a relatively high transfer rate is the evaporation/condensation of water vapour ("latent heat transfer"), and that the temperature profiles of dry air are different from "moist" air[15]. However, the phase changes associated with water are assumed to be the only relevant ones, and they are assumed to mainly alter convective processes.

2.3 Ozone heating theory

The standard explanation as to why the temperature in the tropopause stops decreasing with height and begins increasing with height in the stratosphere is the "*ultraviolet heating*" or "*ozone heating*" theory.

This theory proposes that ultraviolet (UV) light is absorbed by oxygen and ozone in the upper atmosphere where it is converted into heat. This heat then increases the temperature of the air enough to compensate for the energy lost to the gravitational field[5, 6, 16–19]. Because of the popular assumption that hot air always rises, it is then assumed that this energy mostly remains "trapped" above the troposphere.

2.4 Greenhouse effect theory

Another theory which forms a major component of the conventional explanation for atmospheric temperature profiles is the *"greenhouse effect theory"*[11]. This theory proposes that the presence of certain trace gases, known as *"greenhouse gases"* (chiefly

H_2O, CO_2 and O_3), have a major influence on atmospheric temperatures by slowing down the rate of *"infrared cooling"* of the planet[12, 20].

Almost all of the energy in the atmosphere is believed to derive from incoming solar radiation, and this is typically assumed to be exactly balanced by an equivalent amount of outgoing terrestrial radiation[21]. Because the surface temperature of the sun ($\sim$ 6000K) is considerably hotter than the Earth ($\sim$ 288K), the incoming solar radiation is mostly of higher frequencies (ultraviolet/visible/shortwave infra-red) than the outgoing terrestrial radiation (longwave infra-red).

Tyndall, 1861[22] showed that the two main atmospheric gases (O_2 and N_2) are transparent to infra-red radiation, but that the minor gas (H_2O) and many of the trace gases (e.g., CO_2 and CH_4) were capable of absorbing infra-red radiation. The other main atmospheric gas, Ar was not discovered until 1895[23], but like O_2 and N_2 is transparent to infra-red radiation. Therefore, although collision-induced infra-red emission by the main atmospheric gases is possible[24, 25], the absorption and re-emission of the outgoing infra-red radiation from the Earth is assumed by the theory to be dominated by the trace "greenhouse gases"[11–14, 20–22, 26, 27].

3 Experimental observations

In this article, we use weather balloon radiosonde measurements taken from the University of Wyoming, College of Engineering's Department of Atmospheric Science's global database, available at http://weather.uwyo.edu/upperair/sounding.html.

We confined our analysis to radiosonde data from the North American continent in the period 2010-2011, since this is an area with a relatively high density of weather balloon stations, and includes most of the main climatic regions, e.g., continental, coastal, tropical, subtropical, mid-latitude and polar. In order to study the effects of seasonal variation, we analysed all of the North American radiosondes taken on June 21st 2010 and December 21st 2010, i.e., the summer and winter solstices.

For this study, we analysed radiosondes from all of the locations shown in Figure 3. For brevity, in this article we will focus our discussion on a few representative stations (Norman Wells, Baker Lake, Yarmouth, Albany and Lake Charles) - these stations are highlighted in Figure 3. However, our discussion applies to all of the North America stations shown. In the Supplementary Information, we include the radiosonde measurements for all of the 125 stations in Figure 3.

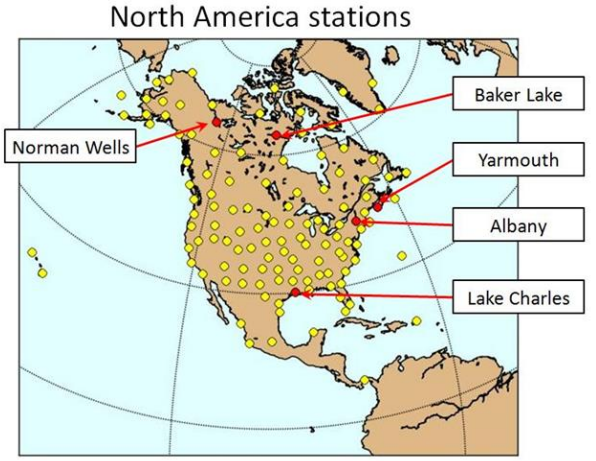

Figure 3: *Locations of the weather balloon stations we analysed for this study. The five stations explicitly discussed in this article are labelled.*

The radiosonde data we studied comprised atmospheric pressure, temperature and relative humidity experimental measurements, as well as several derived variables, e.g., altitude, which were calculated from the experimental measurements. When describing radiosonde profiles, altitude and atmospheric pressure are often considered interchangeable. However, as we will discuss in Section 4.1, the barometric equation used for calculating altitude from pressure (and vice versa) is problematic above the troposphere. So, we will discuss the weather balloon data in terms of barometric profiles (i.e., pressure profiles), instead of altitudinal profiles.

3.1 Analysis of atmospheric profiles in terms of molar density

As discussed in Section 2, some change in the temperature behaviour with altitude occurs at the tropopause. A useful variable for studying atmospheric profiles is the *molar density*, the number of moles per unit volume, D, which we define as,

$$D = \frac{n}{V} \qquad (\text{mol m}^{-3}) \qquad (1)$$

The molar density for an ideal gas can be derived from the ideal gas law. The ideal gas law states that,

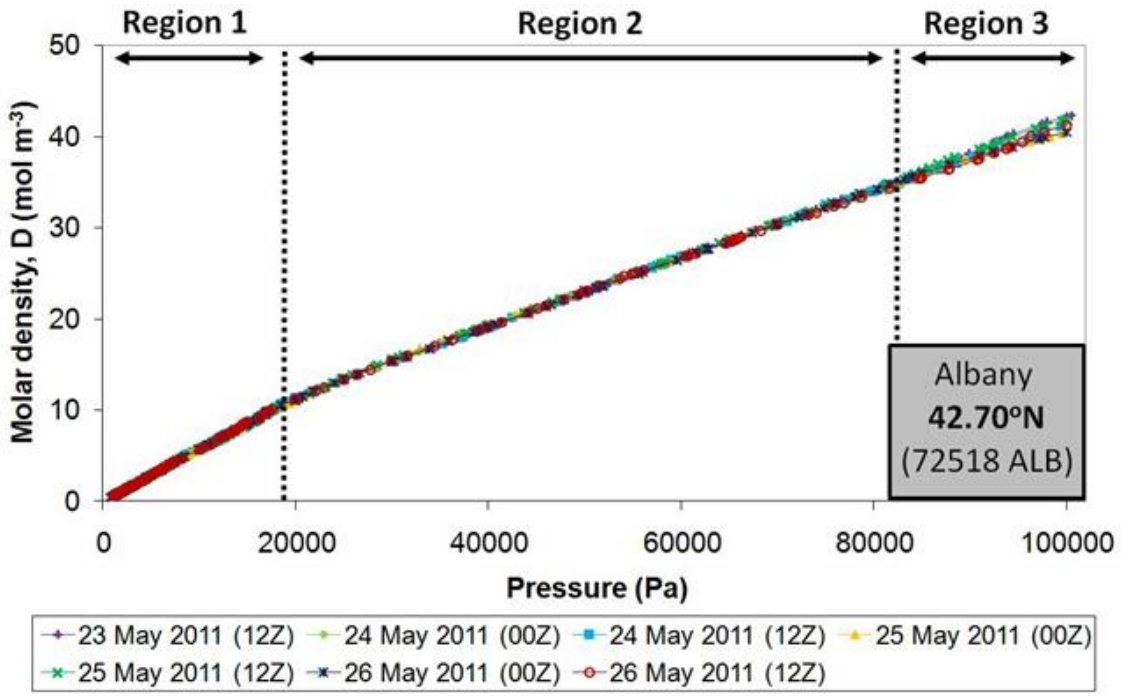

Figure 4: *Plots of specific molar density, D, against pressure, P, for seven consecutive weather balloons launched from Albany, NY (USA) in May 2011. Region 1 corresponds to the tropopause/stratosphere. Region 2 corresponds to the troposphere above the boundary layer. Region 3 corresponds to the boundary layer.*

$$PV = nRT \qquad \text{(J)} \tag{2}$$

Where P is the pressure (Pa), V is the volume (m^3), n is the number of moles, R is the ideal gas constant (8.3145 J K^{-1}) and T is the temperature (K). P and T are both *intrinsic* variables, i.e., their value is independent of the amount of gas present. V and n are both *extrinsic* variables, i.e., their value depends on the amount of gas present. Rearranging Equation 2 gives,

$$\frac{n}{V} = \frac{P}{RT} \qquad (\text{mol m}^{-3}) \tag{3}$$

Hence, from Equation 1, the molar density for the ideal gas can be calculated as,

$$D = \frac{P}{RT} \qquad (\text{mol m}^{-3}) \tag{4}$$

Since P and T are both intrinsic variables and R is a constant, the variable $D = \frac{n}{V}$ is also an intrinsic variable, even though n and V by themselves are both extrinsic variables.

The radiosonde measurements used in this paper include both P and T, and therefore D can be easily calculated from Equation 4. Hence, from the balloon data, the molar densities can be determined over all of the atmospheric profile which is within the range of the weather balloons, i.e., up to where the balloons burst, which is typically about 30-35 km.

Figure 4 shows plots of the change in molar density (D) with pressure (P) for seven consecutive radiosondes taken in 12 hour intervals at an arbitrarily chosen mid-latitude station. The radiosondes were launched from Albany, NY (USA) at 42.70°N, 73.83°W, between 23/05/2011 and 25/05/2011.

Molar density and pressure both decrease with altitude, i.e., they are both highest at ground level, and close to zero in space. Hence, in Figure 4, the right hand side corresponds to ground level molar densities, while the left hand side corresponds to molar densities in the stratosphere.

We can see from Figure 4, that from about 80,000 Pa to about 20,000 Pa, this decrease is linear. Similarly, from about 20,000 Pa to the end of the radiosonde measurements (typically about 1,000 Pa), the decrease is linear. However, the slopes and intercepts of the lines are different in both regions. This is unexpected and indicates some regime change occurs at around 20,000 Pa (for these radiosondes). For

each of the radiosondes, the regime change coincides exactly with the troposphere/tropopause transition for that sonde. We refer to the lower pressure regime as Region 1 and the higher pressure regime as Region 2.

This bi-linear decrease in molar density with pressure occurs for all of the radiosondes we analysed, and three representative examples from other locations on the North American continent are shown in Figure 5. All three of the radiosondes in Figure 5 were launched at the same date and time - 21st June 2010, 12:00 GMT. The pressure at which the regime change occurs varies with latitude (and also season). In general, the change occurs at higher pressures for higher latitudes and colder seasons. It tends to occur at the highest pressures in winter in polar regions and at the lowest pressures in summer at low latitudes.

In all cases, the regime change corresponds to the troposphere/tropopause transition. This suggests that the two phenomena are strongly related. We suggest that they are actually just two aspects of the *same* phenomenon.

It can be seen from Figure 4 that there is a third regime (Region 3) for the Albany radiosondes at high pressures ($>\sim 80,000$ Pa). This region corresponds to the boundary layer, a region which can have relatively high moisture content. Unlike Regions 1 and 2 where the plots of all seven radiosondes are almost identical, in Region 3, the slopes (and intercepts) of the plots are slightly different for different radiosondes. In some cases, the slopes of the lines are the same as for Region 2, but in other cases the slope is either slightly larger or slightly smaller than the slope for Region 2.

From inspecting the associated relative humidity measurements of the radiosondes (see Supplementary Information), it appears that the larger slopes correspond to radiosondes which involved one or more rain events, while the smaller slopes correspond to radiosondes with relatively low humidity conditions in the boundary layer. This suggests that the differences in slopes in Region 3 are water-related. Our brief analysis of these differences indicates many subtle and not-so-subtle phenomena, which are worthy of further investigation. But, for the purposes of this study, we will mostly consider the more abrupt and distinct differences between Regions 1 and 2.

If the changes in slope in Region 3 are associated with water phase changes (e.g., liquid $\Leftrightarrow$ gas), then it seems plausible that the change in slope at the start of the tropopause similarly indicates a change in phase.

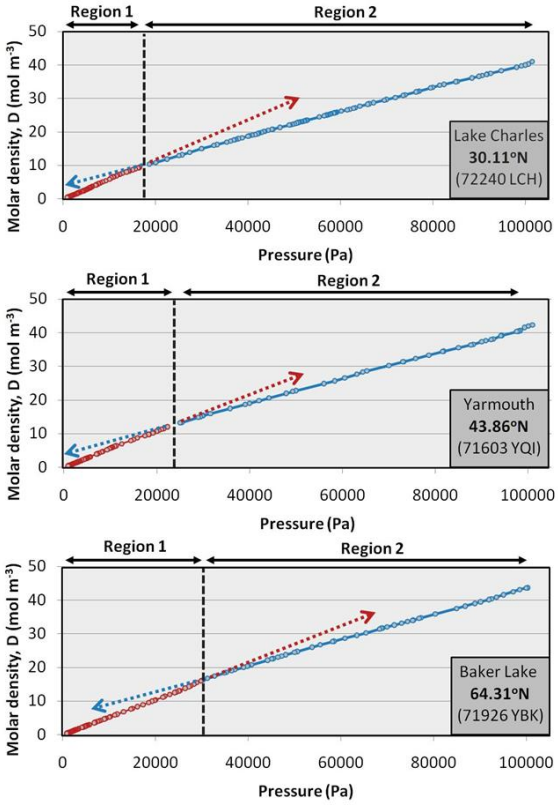

Figure 5: *Typical plots of the change in molar density, D with pressure, P, for weather balloons launched in North America at three different latitudes on 21st June 2010 (12:00 GMT).*

However, this is a dry region and so this phase change cannot be due to water. Indeed, the change in slope at the tropopause is considerably more pronounced than the slope changes in Region 3, which suggests that it involves a substantial change in one or more of the main atmospheric gases, i.e., nitrogen and/or oxygen. We note that the transition could be explained by a change in the mean molecular weight of the air. However, the relative concentrations of nitrogen and oxygen are known to be relatively constant within the troposphere/tropopause/stratosphere regions[1]. Hence, it is unlikely to involve a substantial change in their relative concentration.

In Paper II[2], we propose that this phase change is due to partial multimerization of the atmospheric gases, i.e., an increase in concentration of the so-called "van der Waal" molecules. But, for the purposes of this paper, it is not essential to establish the exact identities of the phases, and so we will simply refer to the Region 1 and Region 2 phases as the

"*heavy phase*" and the "*light phase*" respectively.

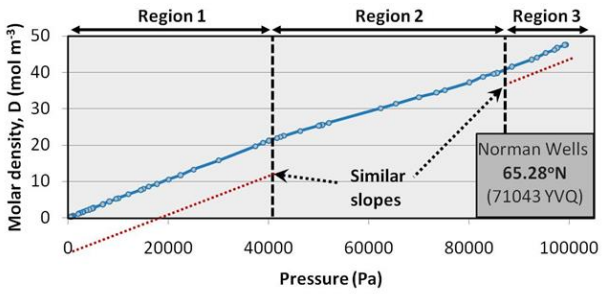

Figure 6: *Typical plot of D and $\Delta D/\Delta P$ versus pressure, P, for a radiosonde taken in the Arctic winter - in this case, 71043 YVG Norman Wells, NT (Canada) on 21st December 2010 (00:00 GMT).*

From studying the molar density/pressure plots for different latitudes and times of year, we note that the behaviour of the boundary layer region for radiosondes taken in the cold Arctic winter is different from those of the other North American radiosondes. Figure 6 shows the plot of D for the radiosonde taken on December 21st 2010 at Norman Wells, NT (Canada)[1]. This radiosonde was taken at a time of very low ground temperatures, typical of the Arctic winters. As can be seen from Figure 6, the slope of the plot of D versus P in the boundary layer is similar to that in region 1 (i.e., the tropopause/stratosphere). As the boundary layer is very dry (<1 g of water vapour/kg air) at these low temperatures, the different slopes are unlikely to be due to water for such radiosondes.

Since the slope of the boundary layer is similar to that in Region 1, i.e., the heavy phase, we suggest that the air in the boundary layer is *also* in the heavy phase, for this case. This means that the heavy phase can exist near ground level as well as in the tropopause/stratosphere under cold, Arctic winter conditions. In Paper II, we suggest that changes in the distribution of this ground level heavy phase influence the so-called *"polar vortices"* found at high latitudes.

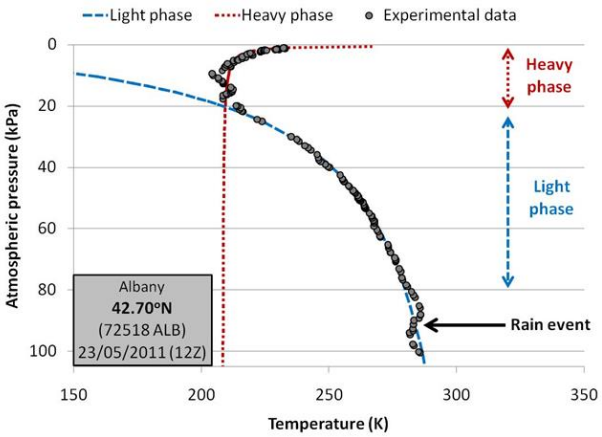

Figure 7: *Comparison of the experimental barometric temperature profile for the 23 May, 2011 (12Z), Albany, NY (USA) radiosonde to a two-phase regime, using Equation 7 and the fitting coefficients listed in Table 2.*

3.2 Fitting barometric temperature profiles

We saw in Section 3.1 that, for a given radiosonde, the different atmospheric regions in a plot of molar density D against pressure P are very well described by straight lines. Hence, for a given region, we can describe the relationship between D and P using the equation of the line, i.e.,

$$D = aP + c \tag{5}$$

where a is the slope and c is the intercept of each line with the D axis. However, while such plots are insightful from a molecular point-of-view, from a meteorological perspective, it might be considered more useful to be able to describe the changes in temperature with pressure for a given radiosonde, i.e., the *barometric temperature profile*.

Since, $D = \frac{P}{RT}$,

$$\frac{P}{RT} = aP + c \tag{6}$$

This can be rearranged to,

$$P = \frac{cRT}{1 - aRT} \tag{7}$$

or

$$T = \frac{P}{aRP + cR} \tag{8}$$

Sonde date	a_1	a_2	c_1	c_2
23 May; 12Z	0.000577	0.000381	-0.06	3.92
24 May; 00Z	0.000580	0.000375	-0.07	4.16
24 May; 12Z	0.000577	0.000378	-0.06	4.00
25 May; 00Z	0.000564	0.000380	-0.01	4.00
25 May; 12Z	0.000564	0.000381	-0.02	3.97
26 May; 00Z	0.000571	0.000380	-0.04	3.87
26 May; 12Z	0.000573	0.000375	-0.05	4.07
Mean	0.000572	0.000378	-0.05	4.00
Standard deviation	0.000006	0.000002	0.02	0.09

Table 1: *Slopes (a) and intercepts (c) of the D:P plots for the seven radiosondes from May 2011 shown in Figure 4. a_1 and c_1 correspond to the linear fit for Region 1, i.e., the tropopause/stratosphere region, while a_2 and c_2 correspond to the linear fit for Region 2, i.e., the troposphere region above the boundary layer.*

Latitude	a	c	**Station**
Humid phase			
30.11°N	0.000348	5.39	Lake Charles
Light phase			
30.11°N	0.000377	3.61	Lake Charles
42.70°N	0.000381	3.92	Albany
65.28°N	0.000390	5.82	Norman Wells
Heavy phase			
30.11°N	0.000593	-0.10	Lake Charles
42.70°N	0.000577	-0.06	Albany
65.28°N	0.000527	0.09	Norman Wells (u)
65.28°N	0.000541	-6.24	Norman Wells (g)

Table 2: *Slopes and intercepts of the fitting functions used for Figures 7 and 8. Lake Charles (72240 LCH) was launched on 21/06/2010 12Z; Albany (72518 ALB) was launched on 23/05/2011 12Z; Norman Wells (71043 YVG) was launched on 21/12/2010 00Z. For the Norman Wells radiosonde, there are two heavy phases, one at ground level (g), and one in the upper atmosphere (u).*

This means that we can use the linear fitting parameters of the D versus P plots to estimate the temperature at a given pressure (or vice versa) in a given atmospheric region. Figure 7 compares such an estimate to the experimentally measured values for one of the Albany, NY (USA) radiosondes in Figure 4 (23 May, 2011 - 12Z). The fit is very good, considering that the entire barometric temperature profile is estimated in terms of just two straight line $D:P$ regions. Slight deviations from the "light phase" region estimates are apparent in the boundary layer (below about 80000 Pa). These appear to be related to changes in humidity, e.g., rain events.

As we noted in Section 3.1, above the boundary layer (Region 3), the D versus P plots are almost identical for all seven of the Albany, NY (USA) radiosondes of Figure 4. As a result, the slopes and intercepts of Regions 1 and 2 are essentially the same for all seven radiosondes (see Table 1), and hence, so are the estimated barometric temperature profiles (not shown).

Table 2 compares the fitting parameters of the Albany radiosonde of Figure 7 to those from a sub-tropical summer radiosonde (Lake Charles, LA, USA; 21 June, 2010; 12Z) and a near-Arctic winter radiosonde (Norman Wells, NT, Canada; 21 December, 2010; 00Z). Together, the three radiosondes are representative of mid-latitude, sub-tropical and Arctic profiles, respectively. Unlike between the seven Albany radiosondes, there is some slight variability in the slopes (a) of the phases between radiosondes at the three different locations (and seasons). However, the variability is remarkably low, even though the radiosondes each were taken at different locations and times of the year, with the a values for all three radiosondes being in the range $0.000377 - 0.000390$ for the light phase and $0.000527 - 0.000593$ for the heavy phase. This indicates that both phases have very distinct barometric temperature behaviours, regardless of location and time of year.

We will discuss the thermodynamic significance of the a constants in the Appendix. In Section 3.4, we will show that a is not quite a constant, but has a temperature dependence. However, the deviation from the constant value for an individual radiosonde, is too small to be detected, because of experimental error. There is also considerable variability in the intercept values (c). We will discuss the variations in c at the end of this section.

In Figure 8, the barometric temperature profiles for the Lake Charles and the Norman Wells radiosondes are compared to their corresponding estimates from Equation 7. Like the Albany radiosonde, the profiles are remarkably well approximated in terms of a very small number (three) of different regions of linear $D:P$ behaviour.

The Lake Charles, LA (USA) weather station is less than 10km from a coastal lake, and less than

[1]Strictly, Norman Wells is not an Arctic station, but with a latitude of 65.28°N, it is close enough to the Arctic circle (> 66.56°N) to be considered "near Arctic".

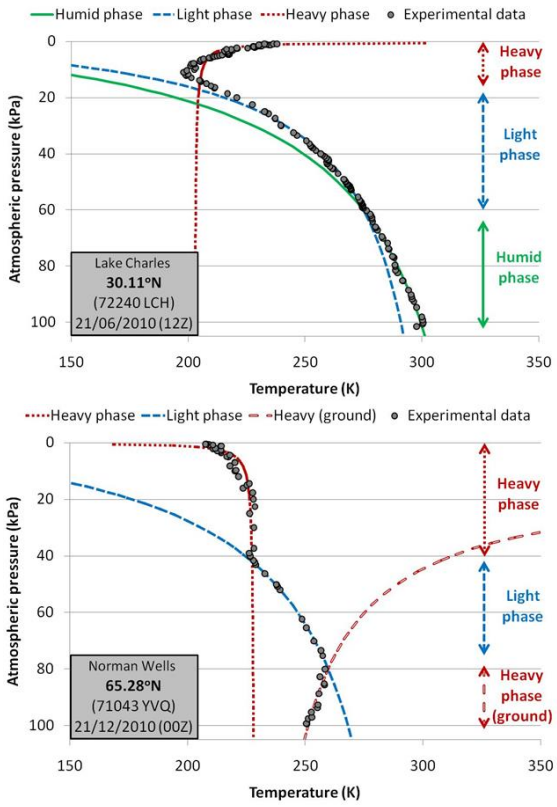

Figure 8: *Comparison of experimental barometric temperature profiles with theoretical estimates determined using Equation 7. The fitting coefficients used are listed in Table 2. Top: a sub-tropical summer radiosonde, Lake Charles, LA (USA); 21 June, 2010 (12Z). Bottom: an Arctic winter radiosonde, Norman Wells, AK (USA); 21 December, 2010 (00Z).*

40km north of the Gulf of Mexico, and hence local air tends to be relatively moist. Also, since it is a subtropical location, the absolute humidity of the air near ground level can be quite high, particularly in the summer when this radiosonde was launched. This is why the boundary layer (defined here as having an absolute humidity of > 1 g of water per kg of air) can reach relatively low pressures (high altitudes), in this case ~ 60000 Pa. Hence, we calculated the slopes and intercepts for this region ("Humid phase") separately from the upper troposphere region ("Light phase").

From Table 2, it can be seen that the slope for the humid phase is slightly lower ($a = 0.000348$) than the light phase ($a = 0.000377$) but the intercept is slightly higher ($c = 5.39$ compared to $c = 3.61$ for the light phase). As can be seen from Figure 8, the actual temperature at ground level (hollow circles) is greater than it would have been for the dry, light phase (dashed, blue line). In other words, the high humidity seems to have increased the ground temperature for this radiosonde.

In contrast, the Norman Wells radiosonde corresponds to very cold (and hence dry) ground temperatures. As noted in Section 3.1, the lower part of the troposphere (up to about 80000 Pa) has a different $D : P$ behaviour from the upper troposphere for this sonde, and hence is treated as a separate atmospheric region, as for Lake Charles. We saw from Figure 6 that the $D : P$ slope of this lower tropospheric region was similar to that in the tropopause/stratosphere, and this is confirmed in Table 2, where the a values are 0.000541 and 0.000527 respectively, compared with 0.000390 for the upper troposphere. This agrees with our suggestion in Section 3.1 that both regions correspond to the air adopting the "heavy phase".

It is remarkable that the barometric temperature profiles are fitted so well using the slope and intercept of just two or three straight line regions obtained from D/P plots. This is unexpected from the conventional explanations for the atmospheric temperature profiles, as summarised in Section 2. In the conventional explanations, the temperature at a given pressure and location is a complex function of the pressure, radiative flux and concentration of greenhouse gases, which varies substantially with altitude. However, Figures 7 and 8 suggest that the changes in temperature with altitude (pressure) correspond to a simple linear relationship between D and P for a given region. Hence, it is worth considering the behaviour of the a and c constants of these linear regions.

3.3 Meteorological significance for different a and c constants

We saw from Figures 7 and 8 that when a $D : P$ linear relationship is converted into a $P : T$ relationship, the barometric temperature profile can actually seem quite complex. Different values of a and c can dramatically alter the $P : T$ profile. So, if you were unaware of the $D : P$ linear relationships, the barometric temperature profile could seem fairly complex, chaotic, and somewhat non-intuitive, i.e., the temperature *seems* to meander up and down from the average "standard atmosphere" profile (Figure 1) almost randomly.

We find that the barometric temperature profiles

become *much* simpler once you recognise the bi-linear (or tri-linear) nature of the barometric molar density profiles, i.e., once you identify the two or three linear $D : P$ relationships for a given profile.

Hence, in this section, it might be useful to briefly discuss how different a and c constants define the barometric temperature profile for a particular regime. Mathematically, the barometric temperature profile for a given a and c is a quite straightforward relationship, i.e., Equations 7 or 8. However, initially, the relationship can seem somewhat non-intuitive, particularly since most of us are used to considering the barometric temperature profile just in terms of P and T.

In the Supplementary Information, we have included a Microsoft Excel file which allows you to view the barometric temperature profile for a given a and c, and then manually alter these values to get a "feeling" for the mathematical relationships of Equations 7 and 8. In this section, we will summarise the main features of these mathematical relationships.

Figures 9, 10 and 11 are schematic plots which illustrate the significance of different a and c constants.

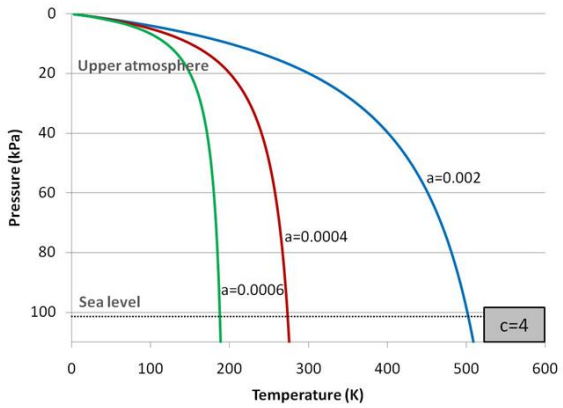

Figure 9: *Effects of varying a, while keeping c constant.*

Figure 9 illustrates how different a values affect the barometric temperature profile. We can see that higher values of a lead to a lower temperature at sea level. It also can be seen that, as pressure increases, the rate of temperature change with pressure (i.e., the *barometric temperature lapse rate*) asymptotically tends to zero. This tendency appears to increase with a. All three plots converge towards low temperatures at low pressures.

Figure 10 illustrates how different c values affect the barometric temperature profile. The $c = 0$ plot shows **no** variation of temperature with pressure, i.e., it implies a barometric temperature lapse rate of exactly zero. Positive c values show a decrease in temperature with pressure, which is the typical behaviour within the troposphere. However, negative c values show increasing temperatures with decreasing pressure, which is the behaviour typically associated with the stratosphere.

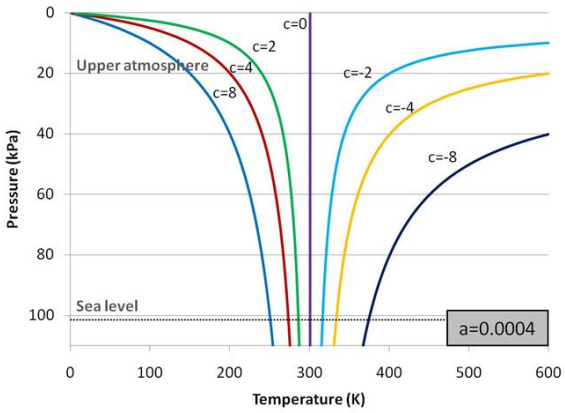

Figure 10: *Effects of varying c while keeping a constant.*

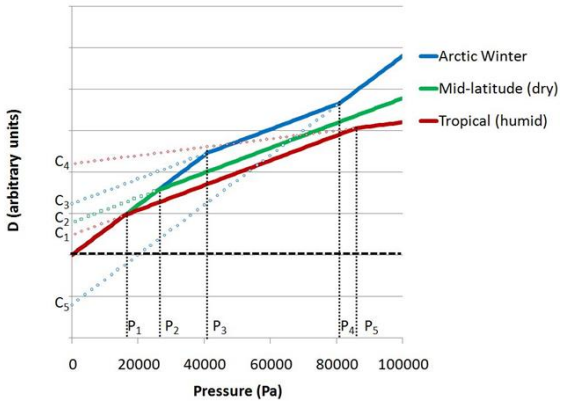

Figure 11: *Dependence of c on the value of a and the pressure, P_c, at which the phase change occurs.*

From Table 2, it can be seen that the c values for the tropopause/stratosphere region are all close to zero, but can be either positive or negative. If the c values are slightly negative, this corresponds to an increase in temperature with decreasing pressure, i.e., "stratospheric heating" (e.g., the Lake Charles and Albany radiosondes). Interestingly, in the Norman Wells case, $c < 0$ for Region 3 corresponding to a *positive* lapse rate in the lower troposphere (Figure 8).

If the c value is slightly positive in the

tropopause/stratosphere (e.g., for Region 1 of the Norman Wells profile), a positive lapse rate does *not* occur. According to the conventional terminology, this would mean that the "stratosphere" is missing for the Norman Wells case, even though the "tropopause" is present.

This is a problem for the conventional ozone heating explanation for the stratosphere/tropopause temperature behaviour which implies that the "pausing" of temperature in the tropopause behaviour is a *reduction* in the amount of "stratospheric heating" at lower altitudes. If the tropopause genuinely was a reduced magnitude version of the stratosphere, then regions without "stratospheric heating" would not have a tropopause either.

However, if the stratosphere/tropopause temperature behaviour is instead related to the phase change, as we suggest, this is no longer a problem. In that case, we can see from Figure 10, that the "pausing" of the tropopause corresponds to a low c value in the upper atmosphere and the sign of the barometric temperature lapse rate in the stratosphere merely depends on the sign of c, i.e., it is possible to have a tropopause even if the lapse rate is slightly negative in the stratosphere.

One might expect that c for the upper phase should be 0, since $D = 0$ when $P = 0$. However, it should be recalled that in this paper, our analysis is limited to the tropospheric to stratospheric regions. From Figure 1 it can be seen that there are other changes in the temperature lapse rates between the stratosphere and space, and hence there are other stages between the stratosphere and outer space. Some of these transitions may similarly involve heavy/light phase changes, but the regions above the stratosphere are beyond the scope of this paper.

Figure 11 is an artificially-generated schematic of D versus P profiles, designed to qualitatively summarise the different behaviours we have observed for the three main climatic regions - Arctic winter, mid-latitude (dry) and tropical (humid). From Equation 4, we know that low temperature/high pressure conditions correspond to high D values. Therefore, D at sea level tends to be highest for cold, high pressure conditions (Arctic winter) and lowest for warm, low pressure conditions (tropical humid).

In theory, D should be zero when $P = 0$. This implies that the slope of the light phase (i.e., a) would be higher for the cold, high pressure conditions than warm, low pressure conditions, since D has further to decrease. This is confirmed from Table 2, since for the light phase, the a constant increases slightly with latitude (Lake Charles < Albany < Norman Wells). However, as seen from Figure 2, the tropopause occurs at lower temperatures and pressures for tropical profiles than polar profiles. So, we would expect this trend to be reversed for the heavy phase. This is also confirmed from Table 2, as a appears to roughly decrease with latitude for the heavy phase (i.e., Norman Wells < Albany < Lake Charles).

The intercept, or c value, for each linear region depends on the pressure at which a phase transition occurs, as well as the type of phase change which occurs. As the phase change from the troposphere to the tropopause usually corresponds to just one type of phase change (i.e., the transition from light phase to heavy phase), the c constant for the upper troposphere is mostly just a function of the pressure at which the phase change occurs. The lower the pressure at which the transition occurs, the closer the intercept is to zero, i.e., c decreases.

For the lower troposphere phase changes, the values of c also depend on the type of phase change. If the phase change is due to water vapour, e.g., a high humidity in the boundary layer, as for the Lake Charles radiosonde, then the c value for the lower troposphere also decreases if the pressure at which the phase change occurs is decreased. However, if the phase change corresponds to a transition from heavy phase to light phase, as for the Norman Wells radiosonde, then the opposite occurs. In these cases, c for the lower troposphere is negative.

3.4 Theoretical and experimental significance of a

In the Appendix, we derive theoretical equations for the a values described in Section 3.2, i.e., the slopes of the lines in the D/P plots,

$$a = \frac{dD}{dP} \tag{9}$$

There we show from thermodynamics that for any mixture of gases,

$$a = \frac{1}{\gamma RT} \tag{10}$$

Where, as defined in the Appendix, γ is the ratio of the total molar energy capacity, C_T to the molar energy capacity at constant volume, C_V, i.e.,

$$\gamma = \frac{C_T}{C_V} \tag{11}$$

Its value depends on the gases, and the type of thermodynamic system the gases are in.

For a mixture of diatomic N_2 and O_2 (i.e., dry air in the light phase), we derived in the Appendix, γ values for three different thermodynamic conditions.

- An isothermal process ($\gamma_i = 1$) $\Rightarrow a_i = \frac{1}{RT}$
- An adiabatic process with no field change ($\gamma_a = 1.4$) $\Rightarrow a_a = \frac{1}{1.4RT}$
- An adiabatic process in a gravitational field ($\gamma_g = 1.2$) $\Rightarrow a_g = \frac{1}{1.2RT}$

As we discuss in the Appendix, γ for air can vary with atmospheric composition, e.g., water content or the presence of heavy phase air. γ can also vary from changes in the interactions between the air and the different energy fields (i.e., gravitational, electrostatic or magnetic), or if energy is lost or gained by the air. A number of processes can result in a volume of air losing or gaining energy - radiative absorption/emission; chemical reactions (e.g., "ozone heating"); phase changes (e.g., condensation/evaporation of water or the light phase/heavy phase transition); etc.

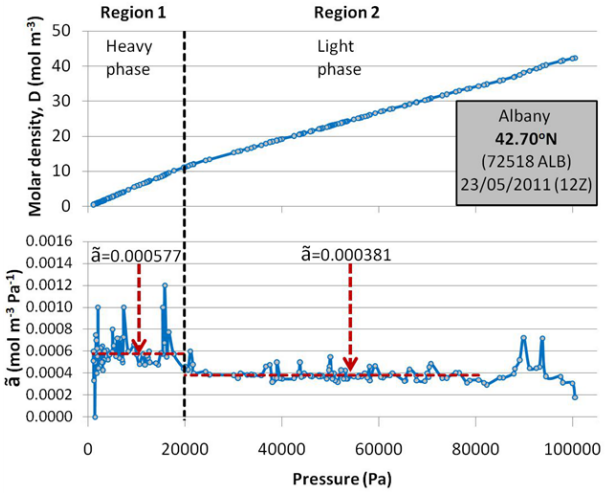

Figure 12: *Comparison of the $D : P$ plots to the corresponding $\widetilde{a}$ plots for the Albany radiosonde data of Figure 7. The dashed red lines correspond to the mean a values for each of the phases, i.e., the fitting parameters used for Figure 7.*

From Equation 10, it can be seen that a should have a temperature dependence. However, in Section 3.2, when calculating the value for a, it was assumed

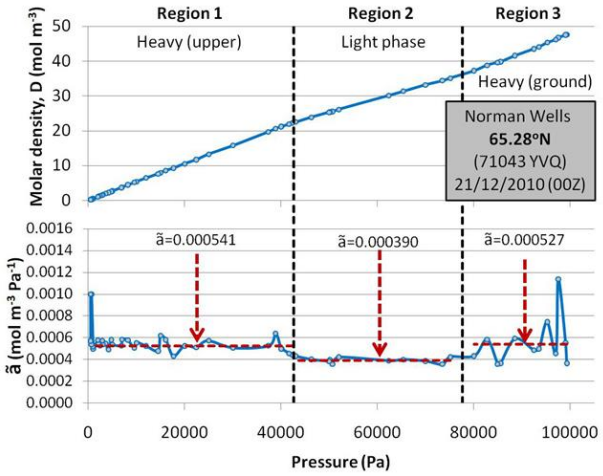

Figure 13: *Comparison of the $D : P$ plots to the corresponding $\widetilde{a}$ plots for the Norman Wells radiosonde data of Figure 8. The dashed red lines correspond to the mean a values for each of the phases, i.e., the fitting parameters used for Figure 8.*

that the D versus P functions were exactly linear for each phase. To investigate the non-linearity of the D versus P functions within each phase, we find it useful to plot $\Delta D/\Delta P$ against pressure, where ΔD and ΔP are the differences in D and P (respectively) between two consecutive measurements from the same radiosonde. Ideally, as ΔP tends to zero, $\Delta D/\Delta P$ becomes equivalent to the derivative of D with respect to P, i.e., the instantaneous slope, a,

$$\lim_{\Delta P \to 0} \frac{\Delta D}{\Delta P} = \frac{dD}{dP} = a \qquad (12)$$

Of course, since radiosondes only record a finite number of measurements, $\Delta P \gg 0$ between consecutive measurements. Nevertheless, we find that the ratio can act as a reasonable approximation of the instantaneous slope at a given pressure. We define this ratio as $\widetilde{a}$,

$$\widetilde{a} = \frac{\Delta D}{\Delta P} \approx a \qquad (13)$$

In Figures 12 and 13 we compare the $\widetilde{a}$ values to the fitted a values (red lines) used for the Albany radiosonde of Figure 7 and the Norman Wells radiosonde of Figure 8, respectively. We first note that $\widetilde{a}$ is indeed well-approximated as being constant for a given phase, i.e., the dashed red lines are reasonable fits. This justifies our conclusion in Section 3.2 that the slopes are constant for individual regions. We also

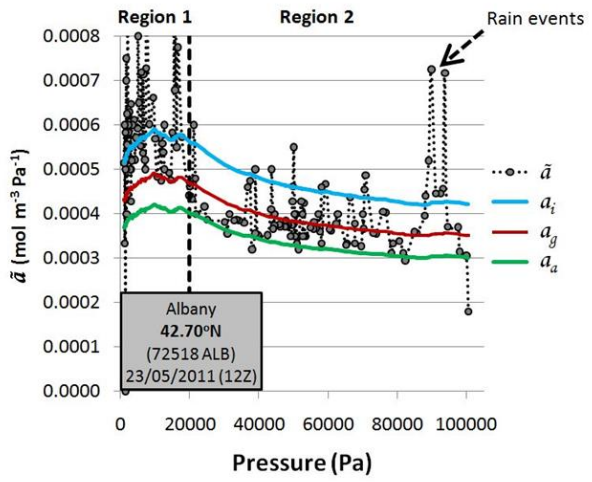

Figure 14: *Comparison of the experimentally-derived $\widetilde{a}$ values to the three theoretical a estimates described in the text, for the Albany radiosonde shown in Figure 12.*

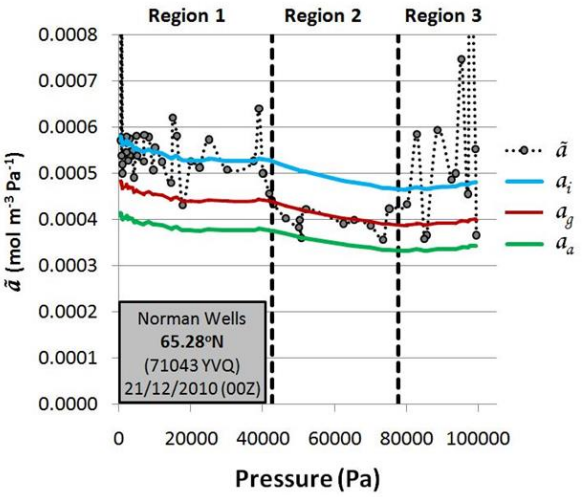

Figure 15: *Comparison of the experimentally-derived $\widetilde{a}$ values to the three theoretical a estimates described in the text, for the Norman Wells radiosonde shown in Figure 13.*

note from Table 1 that the standard deviations for a of the seven Albany radiosondes are all within $\sim 1\%$ of the mean values. This suggests that the mean a values for individual regions of a radiosonde are very well-defined, i.e., the constant slopes corresponding to the mean value of $\widetilde{a}$ are statistically significant.

Despite this, the fits are not exact, and it is plausible that $\widetilde{a}$ does actually have a temperature dependence, as implied by Equation 10. For the temperature profiles observed by radiosondes, the change in temperature is typically quite small over the range of a few kilometres. Hence, the corresponding change in a predicted by Equation 10 would also be quite small

For example, let us consider the change in a predicted by Equation 10 when travelling a vertical distance of 1km. If the lower altitude temperature is $T_1 = 226.5K$ then, with an altitudinal lapse rate of $-6.5K/km$, the temperature 1km higher would be $T_2 = 220.0K$. For dry light phase air in a gravitational field, $a = a_g = \frac{1}{1.2RT}$.

$$\therefore (a_g)_1 - (a_g)_2 = \Delta a_g = 0.000443 - 0.000456 \quad (14)$$
$$= -0.000013$$

The relative change in a_g in moving from T_1 to T_2 is,

$$\frac{\Delta a_g}{(a_g)_1} = \frac{-0.00013}{0.000443} = -0.029 \quad (15)$$

This implies a decrease in a_g of less than 3% per kilometre. For the radiosondes of Figures 12 and 13, the noise of the variability in $\widetilde{a}$ is greater than that.

In Figures 14 and 15, we calculated the theoretical a values predicted for the Albany and Norman Wells radiosondes, for each of our three γ constants, and compared them to the experimental $\widetilde{a}$ values. The theoretical values at each pressure were obtained by simply incorporating the measured T into Equation 10 for a given value of γ.

For the light phase regions (Region 2 in both cases), $\widetilde{a}$ is reasonably well-fitted by the theoretical a_g curve for dry air in the light phase in a gravitational field, provided we exclude the regions associated with rain events.

For the heavy phase regions (Region 1 for Albany, Regions 1 and 3 for Norman Wells), this fit breaks down, and $\widetilde{a}$ instead seems better described by a_i, i.e., the isothermal curve. As we mention in the Appendix, the theoretical isothermal curve does not depend on the molecular composition of the gases, however the curve for a_g does.

Isothermal conditions are often associated with an ongoing phase change. For instance, it is well known that at the boiling point of water, the temperature of the water can remain constant while it is being heated, as the heating provides the latent ("hidden") heat to convert liquid water into gaseous steam. So, if, as we propose, some of the air above the tropopause is undergoing a phase change, this would

explain why the isotropic a_i value would be a better fit for $\widetilde{a}$ above the tropopause.

Near a phase change boundary, rapid fluctuations in the thermodynamic properties of a system often occur, because small changes in temperature or pressure can cause a sudden transition between one phase and the other. If the heavy phase regions are close to the phase change boundary, this could explain why the "noise" of the $\widetilde{a}$ values appears to increase for the heavy phase regions. It also explains the large "spikes" associated with the rain events of the Albany radiosonde. The "noisy" behaviour for the heavy phase is even more pronounced for some of the other radiosondes we examined, but we chose to present the Albany and Norman Wells plots for comparison with the other graphs in this paper.

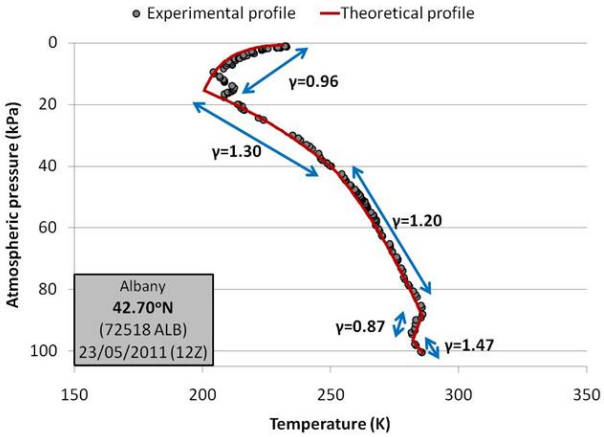

Figure 16: *Comparison of the experimental barometric temperature profile (grey circles) for the Albany radiosonde shown in Figure 12 with a theoretically-derived profile (solid red line), assuming γ adopts the shown values for the regions indicated by the blue arrows, and ground temperature/pressure conditions of 285.75K, 100500 Pa.*

In the Appendix, we show how, given an initial pressure and temperature, and knowing the γ values for each phase, it is possible to generate the barometric temperature profile. A corollary of this is that, we can estimate the appropriate γ values at different pressures for a given radiosonde, by selecting the values which best fit the radiosonde's barometric temperature profile.

Figure 16 compares the experimental barometric temperature profile for the Albany radiosonde of Figure 7 with the calculated temperature profile using the γ values shown on the graph.

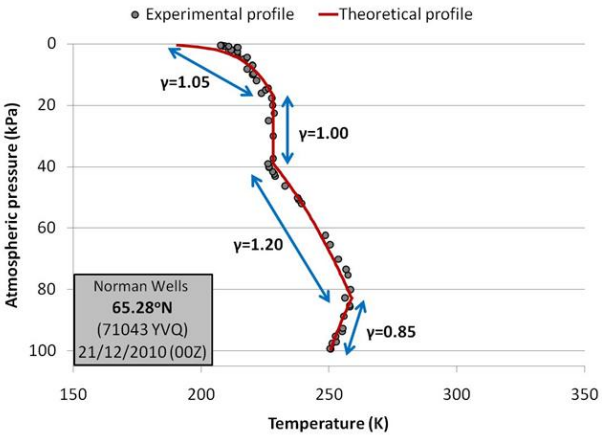

Figure 17: *Comparison of the experimental barometric temperature profile (grey circles) for the Norman Wells radiosonde shown in Figure 13 with a theoretically-derived profile (solid red line), assuming γ adopts the shown values for the regions indicated by the blue arrows, and ground temperature/pressure conditions of 250.65K, 99400 Pa.*

Between 87500 and 41500 Pa, the profile is well fitted by a value of $\gamma = 1.20$, which corresponds to the value predicted for light phase dry air in a gravitational field, i.e., γ_g. However at higher pressures, i.e., in the boundary layer, different values of γ are required for a good fit. We saw from Figures 7, 12 and 14 that this is a region associated with changes in water content. The $\gamma = 0.87$ value from 88500 to 95500 Pa corresponds to a region of 100% humidity. Rain would inject thermal energy into the surrounding air, which at constant pressure, would reduce γ. The low humidity near the ground level would cause the rain from the higher region to evaporate, which will absorb energy from the surrounding air, thus increasing γ to 1.47.

Above 14500 Pa, $\gamma = 0.96$ is required. This approximates $\gamma_i = 1.0$, i.e., isothermal conditions. As we mentioned earlier, phase changes are often associated with isothermal conditions, since the energy gained or lost by the system is typically in the form of latent heat. So the value of $\gamma \approx 1.0$ is probably a result of the light phase/heavy phase transition which begins for this radiosonde at around 14500 Pa. However, we notice that between 40500 Pa and about 20000 Pa, γ is better fit by a value of about $\gamma = 1.3$, rather than $\gamma_g = 1.2$. It may be that the change of phase just above this region has released energy into the air, causing γ to slightly increase.

Figure 17 compares the experimental barometric temperature profile with the calculated barometric temperature profile for the Norman Wells radiosonde of Figure 13, using the γ values shown in the figure.

As for Figure 16, much of the profile (81900 to 38900 Pa) in the upper troposphere is well-fitted by $\gamma = 1.2$. This value corresponds to γ_g, i.e., light phase dry air in a gravitational field. The profile from 37900 to 16900 Pa is well-fitted by $\gamma = 1.0$. We saw from Figures 8, 13 and 15 that the onset of the heavy phase begins at about 40000 Pa for this radiosonde, so again a value close to $\gamma_i = 1.0$ is expected. However, above 16900 Pa, a slightly higher value of γ seems to be necessary. This might indicate the completion of the phase transition, or maybe other factors are involved.

As we discussed earlier, we suggest that the air in the lower troposphere, near ground level, also corresponds to the heavy phase for this radiosonde. However, the value of γ which best fits the profile below about 82900 Pa is 0.85, which is lower than γ for the heavy phase in the upper atmosphere of the profile. If the change in phase at the boundary layer from the heavy to light phase is an endothermic process, then a possible explanation could be that energy is being extracted from the warm boundary layer air to the south. This would reduce γ.

Although much of the analysis of the fitted values of γ for the two radiosondes described above is still speculative, and more research is probably required before we can provide definitive explanations for the γ values of individual regions, we note that the fitted theoretical plots of both radiosondes each only require a few different γ values in order to describe the entire barometric temperature profile. This suggests that the use of γ values to describe the barometric temperature profiles of radiosondes is promising, and may provide us with useful insights in the future. We provide some discussion of the theory behind γ in the Appendix.

We are impressed at how the barometric temperature profiles can be so well-described with only a few different regions, for each radiosonde. Since the γ values associated with each region can be thermodynamically derived, this suggests that, at least over the distances of $\sim 30 - 35km$ covered by an individual radiosonde, the air is mostly in thermodynamic equilibrium. As we will discuss later, this contradicts a key assumption of current atmospheric physics theories, which assume that individual air parcels are only in *local* thermodynamic equilibrium[11].

4 Implications

For this paper, we analysed the atmospheric barometric temperature profiles of a large sample of weather balloon radiosondes launched from the North American continent over the 2010-2011 period. A number of significant results were found:

1. A previously unreported widespread phase change in at least one of the main atmospheric gases was found to be associated with the troposphere-tropopause transition. We dubbed the phase associated with the tropopause/stratosphere regions as the "heavy phase", as opposed to the "light phase" which occurred for most of the troposphere. The heavy phase also appears to occur near ground level during cold Arctic winters. In Paper II, we suggest that the heavy phase involves partial multimerization of oxygen, and possibly nitrogen[2].

2. When the radiosondes were analysed in terms of molar density (D) and pressure (P), an almost linear relationship was found for all radiosondes between D and P for each of the phases. However, the linear relationship was different for the heavy phase compared to the light phase. The linear relationships were almost identical for all of the radiosondes considered, although depending on latitude and season there were some slight differences in the slopes of the lines, and also the pressure at which the transition between the phases occurred.

3. Once linear relationships were determined for each of the phases of a radiosonde, it was possible to estimate the relationship between T and P for that phase, using the slopes and intercepts of the lines. Barometric temperature profiles typically show considerable variability over the range of the radiosondes (i.e., $\sim$0 to 35 km, i.e., troposphere to mid-stratosphere). However, by using the approach we developed, very close fits could be obtained between the experimentally-determined T, P values and the estimated values, even though our estimates only assumed two or three different linear regions.

4. The slopes of the linear regions agree well with our predictions based on the thermodynamics of a simple mixture of O_2 and N_2 in a gravitational field, provided that changes in water vapour concentration and the light phase/heavy

phase transitions are accounted for. This suggests that the barometric temperature profiles of the troposphere are not overly influenced by the concentration of trace gases, such as CO_2.

5. The fact that the barometric temperature profiles are so well-described with only a few different thermodynamic regimes suggests that, over the range of a radiosonde (i.e., $\sim 0 - 35$ km), the air is mostly in thermodynamic equilibrium. Previous approaches to describing barometric temperature profiles have assumed that individual air parcels are only in *local* thermodynamic equilibrium, e.g., Pierrehumbert, 2011[11].

These findings have implications for several different research fields, and we will briefly discuss some of the main ones.

4.1 Problems with radiosonde altitudes

Most radiosonde weather balloons measure the pressure, temperature and relative humidity at different levels in the atmosphere, but do not measure the altitude (height, h). Instead, the heights are *derived* from the pressure measurements using the barometric equation[28],

$$P = P_0 \exp(-Mgh/RT) \qquad \text{(Pa)} \qquad (16)$$

Where P_0 is the atmospheric pressure at sea level and M, the mean molecular weight, is assumed to be 28.9 Daltons for dry air. While the molecular weight is often adjusted to take into account the water content given by the relative humidity, until now it has been assumed that no other changes need to be considered. However, if the heavy phase has a different molecular weight (which would be the case if it involves partial multimerization, as we argue in Paper II [2]), then the calculated heights will be incorrect. The same would also apply if pressures are calculated from measured heights.

Most radiosonde systems (e.g., Vaisala RS80, Vaisala RS90 and Graw DFM-97) only directly measure the pressure, temperature and relative humidity - the altitudes are calculated. Other radiosonde systems (e.g., Sippican MKII and Modern GL-98) measure the altitudes directly, e.g., via a 3D GPS, but then calculate the pressure from Equation 16[29].

Our results therefore imply that the *calculated* data (either heights or pressures, depending on the radiosonde) from most radiosondes may be inaccurate above the troposphere, and also in the troposphere during polar winter conditions. We note that this latter point has implications for aeroplane pilots flying in polar winter conditions if they are relying on barometric gauges for determining their altitude.

In recent years, the World Meteorological Organization have carried out a series of inter-comparisons between barometric and GPS radiosonde systems, e.g., Refs. [29–31]. Da Silveira et al., 2001[29] noted discrepancies between the reported heights and pressures of different radiosonde systems, but assumed that these discrepancies were solely due to different instrument errors. In other words, they did not consider the possibility that the mean molecular weight might change above the troposphere.

Radiosonde manufacturers have been applying new calibrations and conversions to their GPS measurements in an admirable attempt to reduce the apparent *"instrument errors"*. As a result, in more recent studies, the discrepancies between the calculated pressures of different GPS radiosondes have been reduced[30, 31]. This has even led to some groups recommending that GPS radiosondes should not attempt to measure pressure, but instead calculate the pressure from the altitude, to *"reduce the cost of consumables"* (Recommendation 13.2.2.1 of Nash et al., 2006[30]).

Our results suggest that such recommendations are unwise. Doubtless there are instrumental errors in many radiosonde systems, and efforts to minimise these errors should be encouraged. But, heights or pressures calculated from Equation 16 assuming a molecular weight of 28.9 are inaccurate if the molecular weight changes in the heavy phase.

We recommend that radiosonde systems should measure *both* pressure and altitude, particularly when considering the upper atmosphere and/or polar winter profiles. However, since the GPS measurements have been recalibrated partly to remove the discrepancy between GPS-calculated pressures and barometer-measured pressures, there is a danger that these recalibrations have incorporated some of the inaccuracy of Equation 16. Therefore, care should be taken to ensure that GPS altitude measurements are determined completely independently from barometer measurements.

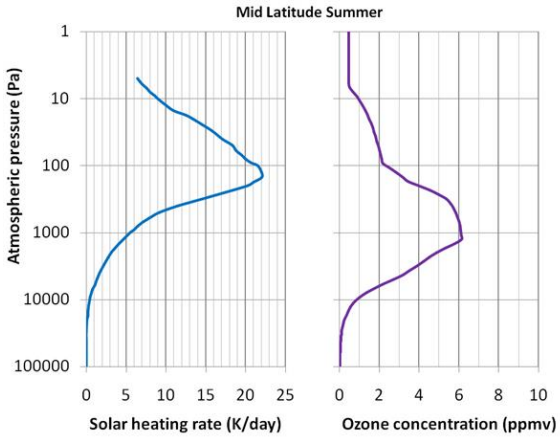

Figure 18: *One modelled estimate of the solar heating rates at different pressures and ozone concentrations, for a mid-latitude summer region. The solar heating rates (left) were estimated from Figure 4 of Chou et al., 1992[16], while the ozone concentrations (right) were taken from the 1990 InterComparison of Radiation Codes in Climate Models (ICRCCM) dataset (test case 27)[32, 33]. The y axis (pressure) is shown as a log scale.*

4.2 Implications for the ozone heating theory

As mentioned in Section 2.3, the conventional explanation for the positive barometric lapse rate in the stratosphere and the close-to-zero lapse rate in the tropopause is based on the "ozone heating" theory. Figure 18 shows a typical model of this proposed ozone heating, obtained from Chou et al., 1992[16]. In these models, the amount of stratospheric heating is usually reported in degrees K (or °C) per day, and is directly related to the amount of incoming ultraviolet radiation absorbed by the atmosphere, i.e., oxygen and ozone.

In general, according to the theory, the higher the concentration of ozone, the more radiation is absorbed, and indeed the absorption of ultraviolet radiation is involved in the formation of ozone. Hence, the modelled *"solar heating rate"* initially increases with increasing ozone concentration. However, as the incoming solar radiation passes through the *"ozone layer"* (a region of the stratosphere with relatively high ozone concentrations), most of the ultraviolet radiation is absorbed, and there is less radiation to be absorbed. So, for the profile in Figure 18, from about 90 Pa, the heating rate starts to decrease with increasing pressure, even though the ozone concentration does not reach a maximum until about 1000 Pa.

According to the theory, by the time the incoming solar radiation has reached the tropopause, the amount of ozone heating has been reduced to the extent that it only just compensates for the energy lost to the gravitational field. This is the theory's explanation as to why the temperature lapse rate is close-to-zero in the tropopause.

One major problem with the ozone heating theory is that it overlooks the fact that the tropopause tends to be most pronounced in the middle of the Arctic winter, when there is no sunlight (and hence no UV), and least pronounced at the lower latitudes (near the equator), where sunlight (and UV) are greatest. This can be seen by comparing the onset of the tropopause for the different profiles in Figure 2. The current theory would require it to be the other way around.

Another problem is that radiosondes can be found in which the temperature lapse rate is close-to-zero in the tropopause, but slightly negative in the stratosphere (e.g., see Figure 8). If the "pausing" of the tropopause is due to a reduction in the level of ozone heating as the troposphere is approached, then this should not occur.

Our alternative explanation for the tropopause/stratosphere temperature behaviour is based on the previously-overlooked light phase/heavy phase transition. In all of the radiosondes we analysed, the troposphere/tropopause transition coincided with the transition between the light phase and the heavy phase. This suggests that the two phenomena are related. Our analysis shows that such a phase change is sufficient to explain much (if not all) of the tropopause/stratosphere temperature behaviour.

Our theory explains how the tropopause can occur during the Arctic winters - the change in temperature behaviour can occur without sunlight. It allows for atmospheric profiles in which the tropopause has a non-negative temperature lapse rate, even if the lapse rate is slightly negative in the stratosphere above. It can also explain the positive temperature lapse rates at ground level during Arctic winters ("temperature inversion layers"), i.e., temperatures at ground level can become low enough during Arctic winters for some of the air to form the heavy phase (e.g., see Figure 8).

It seems clear that the oxygen and ozone in the ozone layer does absorb a significant fraction of the

incoming solar radiation. For instance, most of the higher frequency ultraviolet light (e.g., above 280 nm) which is present in the incoming solar radiation does not reach the troposphere, i.e., it is absorbed by the atmosphere at higher altitudes[2]. However, if this absorbed energy is then distributed throughout the atmosphere, then it would not necessarily remain in the tropopause/stratosphere. In other words, absorption of ultraviolet radiation in the ozone layer does not necessarily lead to stratospheric heating.

4.3 Implications for the greenhouse effect theory

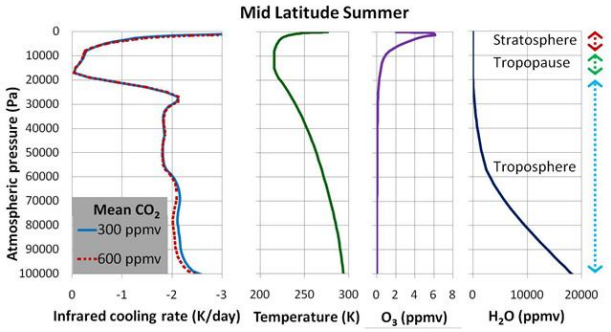

Figure 19: *Modelled estimates of the infra-red cooling rates predicted by the greenhouse effect theory for a mid-latitude summer atmosphere. Data is taken from test cases 27 (300 ppmv CO_2, blue solid line) and 28 (600 ppmv, red dashed line) from the 1990 InterComparison of Radiation Codes in Climate Models (ICRCCM) dataset[12, 32, 33]. Both test cases assume the shown barometric temperature profile (second from left) and H_2O and O_3 atmospheric concentrations (two rightmost panels).*

Our results suggest that the magnitude of the so-called "greenhouse effect"[11–14, 20–22, 26, 27] is considerably less than had previously been assumed, and is probably negligible. Since the greenhouse effect theory is currently a major component of global climate models[11–14, 21, 26], it is worth considering this implication in detail.

According to the greenhouse effect theory (see Pierrehumbert, 2011[11] for a concise summary), barometric temperature profiles are strongly influenced by the presence of trace greenhouse gases (e.g., H_2O, CO_2, O_3 and CH_4) in the atmosphere. Greenhouse gases are assumed to substantially increase the mean temperature of the troposphere and decrease the mean temperature of the stratosphere. Specifically, the theory predicts that the greenhouse gases present in the atmosphere reduce the rate at which outgoing infra-red radiation leaves the Earth into space, i.e., the rate of *infra-red cooling*.

In the theory, the rate of infra-red cooling is believed to vary substantially throughout the atmosphere, with the rate at each location depending on a number of factors: the local concentration of the different greenhouse gases, the local temperature of the air, the atmospheric pressure, as well as the radiative flux passing through that location. The spectrum of the radiative flux at each location is also considered important - if a particular frequency of radiation has already been absorbed before reaching the air parcel, that frequency is said to be *saturated*, and is no longer available to be absorbed by greenhouse gases. Figure 19 shows a typical radiation model for a mid-latitude summer atmosphere, taken from the 1990 InterComparison of Radiation Codes in Climate Models (ICRCCM) dataset[12, 32, 33], which is based on the greenhouse effect theory.

It can be seen from the infra-red cooling model of Figure 19 that the greenhouse effect theory predicts a strong influence from the greenhouse gases on the barometric temperature profile. Moreover, the modelled net effect of the greenhouse gases on infra-red cooling varies substantially over the entire atmospheric profile.

However, when we analysed the barometric temperature profiles of the radiosondes in this paper, we were unable to detect *any* influence from greenhouse gases. Instead, the profiles were very well described by the thermodynamic properties of the main atmospheric gases, i.e., N_2 and O_2, in a gravitational field. The only major deviations were related to the light phase/heavy phase transitions and to changes in water vapour concentrations. While water vapour is a greenhouse gas, the effects of water vapour on the temperature profile did not appear to be related to its radiative properties, but rather its different molecular structure and the latent heat released/gained by water in its gas/liquid/solid phase changes.

For this reason, our results suggest that the magnitude of the greenhouse effect is very small, perhaps negligible. At any rate, its magnitude appears to be too small to be detected from the archived radiosonde data.

[2]High frequency ultraviolet light is harmful to most known life, which suggests that life on Earth evolved without much exposure to high frequency ultraviolet light.

This prompted us to ask what is wrong with the greenhouse effect theory. A critical assumption of the theory is that the air molecules are only in *local* thermodynamic equilibrium, i.e., that a given air parcel is in thermodynamic equilibrium with itself, but is thermodynamically isolated from neighbouring air parcels. As a result, if an air parcel gains more energy than it loses through radiation (or vice versa), energy imbalances between neighbouring air parcels can develop - see Pierrehumbert, 2011[11], for example.

Our results contradict this assumption of local thermodynamic equilibrium. The barometric temperature profiles are very well described by only a few different thermodynamic regimes up to the altitudes reached by current weather balloons (i.e., ~ 35 km). This suggests that the air is mostly in thermodynamic equilibrium. If neighbouring air parcels were thermodynamically isolated from each other, and the major energy imbalances between neighbouring air parcels proposed by the greenhouse effect theory existed, many more thermodynamic regimes would be needed for a good fit.

In Paper III[3], we propose a mechanism by which this thermodynamic equilibrium could easily be maintained over the distance from the ground to the mid-stratosphere (~ 35km). We identify a mechanism for mechanical energy transmission that was not considered by the greenhouse effect theory, which we call *"pervection"*. We find that pervection can be several orders of magnitude faster than the three conventional heat transmission mechanisms of conduction, convection and radiation.

While mechanical energy transmission is not a direct heat transmission mechanism, due to the law of conservation of energy, heat is equivalent to mechanical energy. This means that pervection can rapidly distribute energy throughout the atmosphere over distances of hundreds of kilometres. So, this may explain why the local energy imbalances predicted by the greenhouse effect theory do not appear to last long enough to form a greenhouse effect.

The theory of *"anthropogenic global warming"* (or *"man-made global warming"*) explicitly assumes that the magnitude of the greenhouse effect is substantial for the Earth's atmosphere, in order to reach the conclusion that a doubling or trebling of the atmospheric concentration of carbon dioxide can have a major effect on atmospheric temperatures, even though carbon dioxide would still remain a trace gas[11, 13, 14, 20, 21, 26, 27]. However, if the magnitude of the greenhouse effect is as small as our results imply, the anthropogenic global warming theory would be invalid. In recent decades, the theory has led to considerable public concern over the increase in atmospheric carbon dioxide since the 19th century[34, 35]. So, our analysis of the greenhouse effect theory might have important societal implications.

The greenhouse effect theory also forms a major basis for much of the current calculations of the planetary temperature profiles of other planets[36, 37], a topic which is gaining renewed interest with the increase in recent years[38] of the number of identified "*extra-solar*" planets, i.e., planets in other solar systems. For this reason, our results may be of interest to some astronomers.

4.4 Theories for the effects of solar variability on climate

There have been many studies either proposing or disputing different possible links between solar activity and the Earth's climate - see Refs. [39–42] for some recent reviews of the literature. Unfortunately, the available data is currently quite limited, and often ambiguous, for estimating what trends (if any) there have been in solar activity. Hence, there is a wide range of estimates of solar activity trends, particularly for recent decades. For example, with regard to mean decadal solar activity since the late 1970s (when satellite monitoring became possible), some groups have argued there has been an increase[43], some groups argue there has been a decrease[44], while other groups argue that it has been relatively constant[45].

Nonetheless, there is a general agreement that the variation in the total energy of the incoming solar radiation (*Total Solar Irradiance*) has been less than 0.1% since satellite measurements began[46–49]. This would appear to suggest that changes in the Total Solar Irradiance in recent decades have been almost negligible, and it is therefore hard to see how it could have played much of a *direct* role in recent climate change.

Several researchers have suggested potential mechanisms whereby slight variations in solar activity could indirectly lead to substantial variations in tropospheric climate, e.g., if cosmic rays play a significant role in cloud formation, then slight changes in the solar wind could have a substantial influence on global cloud cover. Ref. [40] reviews some of these proposed mechanisms. However, the apparent evi-

dence for each of these mechanisms is often ambiguous, and as a result has so far been controversial, e.g., see Refs. [39–42].

Other researchers have noted that, while the total energy of the incoming solar radiation has been relatively constant during the satellite era, the spectrum of the incoming radiation is not constant, and there has been considerable variability for the higher frequency ultraviolet wavelengths[46–49].

Several studies have reported strong correlations between solar activity and various *stratospheric* weather patterns, e.g., see Refs. [50–56]. Haigh and others[47–50] have suggested that the variability in the ultraviolet frequencies (and indirectly ozone concentrations) could alter the rate of ozone warming in the stratosphere, thereby offering a potential mechanism by which solar variability could significantly alter stratospheric weather. Changes in stratospheric weather are then thought to indirectly influence tropospheric weather. But, because there is a general perception that the stratosphere is mostly isolated from the troposphere, this indirect influence is assumed to be slight or controlled by complex circulation patterns confined to specific areas[57], e.g., the tropical tropopause layer[5, 6] or the Brewer-Dobson circulation in the Arctic[7, 8].

As we mentioned in Section 4.2, our results show that the ozone heating explanation for the positive temperature lapse rate in the stratosphere is invalid. This initially appears to contradict the current theories as to how solar variability could influence tropospheric climate via stratospheric climate. However, our results actually simplify the potential mechanisms necessary. They show that the barometric temperature profiles of both the troposphere and the tropopause/stratosphere regions are actually highly interconnected. Hence, an energetic change in one region directly influences the other regions, i.e., it is no longer necessary to invoke complex circulation patterns to explain an energy transfer between the stratosphere and the troposphere (or vice versa).

This means that, even though the absorption of the incoming ultraviolet radiation mostly takes place in the stratosphere, once the absorption has occurred, the energy is rapidly distributed throughout the atmosphere. Therefore, the higher solar variability in the ultraviolet frequencies[46] could be directly influencing tropospheric climate.

There is an additional implication of our results for current theories on the effects of solar variability on climate. One of the main correlations between solar activity and stratospheric weather which has been reported is an apparently strong correlation between solar activity and the geopotential height at which the atmospheric pressure reaches 3000 Pa (lower stratosphere)[51, 52]. However, as we mentioned in Section 4.1, the barometric equation used for calculating geopotential height from atmospheric pressure (or vice versa) implicitly assumes the atmosphere is entirely in the light phase. If the ultraviolet variability influences the formation of the heavy phase then this could also influence the *calculated* geopotential heights for 3000 Pa. Hence, much (if not all) of the apparent variability in the 3000 Pa geopotential height may arise from variations in the amount of the atmosphere in the heavy phase.

4.5 Relevance for meteorology

As discussed in Section 3.2, by calculating the D:P ratios for a given radiosonde, we were able to derive very reasonable approximations for the barometric temperature profiles of those radiosondes in terms of only a few values (a and c constants for each phase). This substantially simplifies descriptions of barometric temperature profiles, and therefore should be a very useful tool for meteorologists in describing current weather conditions.

In this article, we briefly assessed the main characteristics of the $D:P$ profiles for a sample of radiosondes launched during the 2010-2011 period. However, we anticipate that further research will provide more insight into the factors which influence the profiles, and their relevant contributions (humidity, solar activity, clouds, etc.) If so, this could lead to significant advances in meteorology, especially if robust relationships between $D:P$ profiles and other weather parameters (e.g., winds, humidity or precipitation) could be determined. Such features could also be included in global climate models.

A high priority for understanding the $D:P$ profiles will be a comprehensive assessment of the identity of the "heavy phase" and the factors involved in its formation and distribution. With this in mind, in Paper II[2], we carry out such an investigation, and we conclude that the heavy phase corresponds to a partial multimerization of the O_2 and/or N_2 molecules in the air.

In the boundary layer, the water phase transitions play a dominant role, and this strongly influences the temperature profile near ground level. Hence, a more detailed analysis of the role that water plays in the $D:P$ profiles should also be a high research priority.

The existence of the previously-overlooked heavy phase may also provide insight into several meteorological phenomena. The jet streams are an important type of circulation system which consist of narrow bands of fast, meandering winds that encircle the globe and are found in the troposphere just below the tropopause. There are two of these streams in each hemisphere - the sub-tropical jet streams (located between the tropics and mid-latitudes) and the polar jet streams (located between the poles and mid-latitudes). The location of these jet streams appears to significantly influence tropospheric weather, through "atmospheric blocking"[58–61].

We note two important characteristics of the jet streams which suggest they are related to heavy phase formation. First, the location of the jet streams are just below the onset of the tropopause, and the exact altitude of the jet streams varies with the tropopause height above the streams[62]. This suggests that the jet streams are strongly related to the onset of the tropopause. We argue that the onset of the tropopause coincides with a transition from the light phase to the heavy phase. Therefore, it seems likely that the jet streams are related to the light phase/heavy phase transition. Second, the location of the subtropical and polar jet streams are characterised by changes in ozone distribution[62]. In Paper II[2], we suggest that the heavy phase is involved in the formation of ozone. If the jet streams are related to the distribution of heavy phase air, then this could explain the correlation between ozone and the jet streams.

Weather observers have noticed since the 18th century that winter temperatures in Greenland are often anti-correlated to those in northern Europe[63]. This anti-correlation appears to be related to the paths adopted by the North Atlantic jet stream[58]. It also appears to influence winter temperatures for much of the northern hemisphere and to be associated with variability patterns in atmospheric pressure distributions such as the *"North Atlantic Oscillation"*[63].

It is believed that a strongly negative phase of the North Atlantic Oscillation (and the related *"Arctic Oscillation"*) is primarily responsible for the unusually cold winters of 2009-10 and 2010-11 in Europe, Russia and the U.S.[64–67]. Hence, if the North Atlantic jet stream is related to the distribution of heavy phase air, changes in the heavy phase distribution could lead to significant climate change.

Some groups have suggested that the strongly negative phase of the North Atlantic and Arctic Oscillations may be related to reductions in Arctic sea ice extent[68] and/or changes in solar activity[69, 70]. If so, then it may be worth investigating how these phenomena would affect the heavy phase distribution.

In Paper II, we propose that the heavy phase involves the partial multimerization of the oxygen and nitrogen molecules in the atmosphere[2]. If our proposal is correct, then we suggest that the formation/destruction of multimers near the phase change boundary would cause air masses to move, i.e., would introduce wind circulation patterns. In Paper II, we discuss how multimerization is involved in the formation of tropical cyclones, and more generally, contributes to cyclonic and anti-cyclonic conditions.

We note that variations in the amount of heavy phase air near ground level during Arctic winters could also influence sub-polar winter weather. Since the heavy phase is denser than the light phase, when air adopts the heavy phase it might displace the light phase air below it, altering local atmospheric circulation patterns. In Paper II, we suggest that changes in this ground level heavy phase lead to polar vortex conditions[2].

This mechanism may also have relevance for understanding long-term climate changes, such as the transitions between glacial and interglacial periods. A number of researchers have proposed that the additional large ice-sheets and glaciers present in the Arctic circle during glacial periods can act as temporary "mountains", leading to large-scale changes in atmospheric circulation patterns[71–74]. These changes in atmospheric circulation could act as feedback mechanisms, either slowing down or speeding up the growth or retreat of the glaciers[71, 72]. We postulate that these glaciers and ice-sheets could also prevent dense heavy phase air from moving in certain directions. This could alter local air temperatures near the ground, and thereby could offer an additional feedback mechanism between the atmospheric circulation and the ice-sheet distributions.

Courtillot et al., 2007[75] found several possible correlations between changes in the Earth's magnetic field (*the geomagnetic field*) and climate. In addition, Scafetta, 2012 noted a correlation between global surface temperatures and the frequency of mid-latitude aurorae[76]. Aurorae are phenomena which occur from an interaction between the atmosphere and the geomagnetic field (they are also related to solar activity[77]), and so Scafetta's study also suggests that variations in the geomagnetic field are correlated to climate variations.

In Section 4.4, we noted the possibility that the heavy phase formation and distribution could be strongly influenced by solar activity. We have also discussed above some mechanisms by which the heavy phase distribution could strongly influence weather patterns. The heavy phase distribution and formation may also be influenced by the geomagnetic field. In Paper II[2], we argue that the heavy phase involves the partial multimerization of O_2. If this is correct, then this is significant because monomeric O_2 is usually paramagnetic, but several of the oxygen multimer species ($(O_2)_n$) are diamagnetic.

The magnitude of the interaction between the geomagnetic field and paramagnetic gases is considerably greater than with diamagnetic gases (as well as being of the opposite sign). Hence, it is plausible that the geomagnetic field could cause the movement of monomeric O_2 from one region to another and/or alter the energy of formation of multimeric $(O_2)_n$. In this way, the geomagnetic field could influence the distribution and/or formation of the heavy phase[3]. If so, this suggests a number of different mechanisms by which geomagnetic variability could be influencing climate, e.g., perhaps these geomagnetic effects play a role in the location of the jet streams discussed above. In this context, we note there has been some suggestion that the North Atlantic Oscillation is influenced by geomagnetic activity[78].

Finally, we note that the other main atmospheric gas, N_2, is also diamagnetic, and so if the geomagnetic field transports paramagnetic O_2 from one part of the atmosphere to another, it is possible that this could modify the $O_2 : N_2$ ratios of the two regions. However, the maximum seasonal variations in the $O_2 : N_2$ ratios near atmospheric measurement stations are only of the order of $\sim 0.01\%$[79, 80].

5 Final remarks

By applying new approaches to analysing the atmospheric profile measurements of weather balloon radiosondes, we were able to identify a previously-overlooked phase change which appears to be responsible for the change in temperature behaviour associated with the transition from the troposphere to the tropopause/stratosphere. This phase change also seems to occur in the lower troposphere during Arctic winters. We refer to the tropopause/stratosphere phase as the *"heavy phase"* and the conventional (non-Arctic winter) tropospheric phase as the *"light phase"*.

Our analysis also highlighted serious problems with two of the radiative physics-based theories currently used by global climate models - the ozone heating explanation for the tropopause/stratosphere temperature behaviour and the greenhouse effect theory.

In a series of companion papers, we investigate these issues further. In Paper II, we consider the identity of the heavy phase, and suggest that it involves the partial multimerization of the oxygen (and possibly nitrogen) in the air[2]. In Paper III, we identify a mechanism for *mechanical energy transmission* in the atmosphere which does not appear to have been considered. We refer to this mechanism as *"pervection"* (in contrast to *con*vection). Our laboratory measurements of pervection show that it can be considerably faster than radiation, convection or conduction[3]. This could explain why the radiative-convective models which currently comprise the core physics of the global climate models[9] are inadequate.

Our findings seem to have a large number of significant implications, which we have attempted to summarise in Section 4. In terms of the current understanding of climate science, a considerable portion of the literature may now need to be revisited (see the 2007 reports by the Intergovernmental Panel on Climate Change for a detailed review of the current literature[26]). In particular, the problems we have identified with the current global climate models appear serious enough to require re-development "from scratch" (see Edwards, 2011[9] for a good review of the development of the current climate models and Neelin, 2011[81] for a good introductory textbook on how they work). Nonetheless, we believe that our new approaches to understanding the physics of the Earth's atmosphere provide more insight, and ultimately should improve attempts at weather prediction and our understanding of climate change.

Acknowledgements

No funding was received for this research.

We are grateful to the University of Wyoming, College of Engineering's Department of Atmospheric Science for publicly archiving global radiosonde measurements at http://weather.uwyo.edu/upperair/sounding.html, as this study was based on data from that archive.

We received some helpful feedback from Don Zieman, Dr. David Matthews and Dr. Lorraine Nolan

[3]Indeed, perhaps, the paramagnetism of the oxygen may itself exert some influence on the geomagnetic field.

on an early draft of this paper.

Appendix. Thermodynamic significance of a

In this appendix, we will attempt to clarify the thermodynamic significance of the slopes of the lines in the D/P plots, i.e., the a values described in Section 3.2,

We will do this in terms of the *compressibility of gases*. The compressibility of a gas is normally defined as the relative change in volume as a result of a change in pressure, i.e.,

$$dP = -B\frac{dV}{V} \tag{17}$$

Where B is called the *bulk modulus*. However, it is possible to relate B to a, if we consider B in terms of the density of the gas, ρ, which is related to the molar density, D, by

$$\rho = MD \tag{18}$$

Where M is the molecular weight of the gas (Daltons).

The density, ρ, is the mass of gas per unit volume, i.e.,

$$\rho = \frac{nM}{V} \tag{19}$$

If we assume that there is no phase change and that the compression is applied to a fixed amount of gas, then n and M can be treated as constants when calculating the derivative with respect to V, i.e.,

$$\frac{d\rho}{dV} = (nM)\cdot\frac{-1}{V^2} = -\frac{nM}{V}\cdot\frac{1}{V} = -\rho\frac{1}{V} \tag{20}$$

$$\therefore \frac{d\rho}{\rho} = -\frac{dV}{V} \tag{21}$$

But, since $dP = -B\frac{dV}{V}$, we also have,

$$\frac{dP}{B} = -\frac{dV}{V} \tag{22}$$

$$\therefore \frac{dP}{B} = \frac{d\rho}{\rho} \tag{23}$$

$$\therefore \frac{d\rho}{dP} = \frac{\rho}{B} \tag{24}$$

Combining this with Equation 18, we obtain,

$$\frac{d(MD)}{dP} = \frac{MD}{B} \tag{25}$$

If M is constant,

$$M\cdot\frac{dD}{dP} = \frac{MD}{B} \tag{26}$$

$$\therefore \frac{dD}{dP} = \frac{D}{B} \tag{27}$$

Hence, from Equation 9,

$$a = \frac{D}{B} \tag{28}$$

We now have a thermodynamic relationship between a and B, although it is still dependent on D. B can be determined in terms of energy capacities. In general, energy capacities, C, are defined as,

$$C = \frac{dE}{dT} \tag{29}$$

Where E is energy.

For a gas,

$$B = \gamma P \tag{30}$$

where γ is a constant which relates the total energy capacity (C_T) for a mole of gas to the internal (or constant volume) molar energy capacity of the gas (C_V), i.e.,

$$\gamma = \frac{C_T}{C_V} \tag{31}$$

Since $D = \frac{n}{V}$, Equation 28 becomes,

$$a = \frac{n}{VB} \tag{32}$$

But, since $B = \gamma P$ and $PV = nRT$,

$$a = \frac{n}{\gamma PV} = \frac{n}{\gamma nRT} \tag{33}$$

$$\therefore a = \frac{1}{\gamma RT} \tag{34}$$

In other words, we now have a direct relationship between a and γ.

The value of γ depends on the type of process associated with the compression. We will now consider some of these processes.

For an *isothermal* process where only kinetic energy is involved (e.g., at constant volume), $C_T = C_V$. Therefore, the γ constant for an isothermal process is $\gamma_i = 1$.

For an adiabatic process, which does not involve changes in field energy or phase, the total energy capacity has an additional energy capacity due to the work component ($\frac{d(PV)}{dT}$),

$$C_T = C_V + \frac{d(PV)}{dT} \tag{35}$$

From the ideal gas law[4], $\frac{d(PV)}{dT} = R$. Hence,

$$C_T = C_V + R \tag{36}$$

In this case, $C_T = C_P$, the adiabatic molar energy capacity.

From the kinetic theory of gases, we can calculate C_V using the concept of degrees of freedom. The number of degrees of freedom (α) that a mole of gas has refers to the number of independent modes (or ways) in which the gas can have energy, e.g., translation, rotation and vibration[5]. The energy for each degree of freedom of a mole of gas is $\frac{1}{2}RT$. The total internal energy of a mole of gas at constant volume is usually denoted as U and is equal to the sum of the energy of all of the occupied degrees of freedom, i.e.,

$$U = \frac{1}{2}\alpha RT \tag{37}$$

From Equation 29

$$C_V = \frac{dU}{dT} = \frac{1}{2}\alpha R \tag{38}$$

where $E = U$.

Therefore, for the adiabatic case, we obtain from Equation 36,

$$C_T = (\frac{1}{2}\alpha R) + R \tag{39}$$

$$\therefore \gamma = \frac{\frac{1}{2}\alpha R + R}{\frac{1}{2}\alpha R} = \frac{\alpha + 2}{\alpha} \tag{40}$$

For a mono-atomic gas, $\alpha = 3$ (corresponding to the three translational degrees of freedom). For the diatomic gases N_2 and O_2, at room temperature, $\alpha \approx 5$, but increases slightly with temperature. This is because, in addition to the three translational degrees of freedom, diatomic molecules also have two rotational and a vibrational degree of freedom, but the vibrational degree of freedom is mostly unoccupied at room temperatures.

Therefore, for a diatomic N_2/O_2 mixture (i.e., dry air in the light phase), the γ constant for an adiabatic process is,

$$\gamma_a = \frac{7}{5} = 1.4 \tag{41}$$

However, the Earth's atmosphere interacts with the Earth's gravitational field. So, for a process that involves interaction with the gravitational field, the total energy capacity of the gas also has a gravitational energy capacity component which needs to be considered.

Since only the vertical translational degree of freedom directly interacts with the gravitational field, it is the only degree of freedom that we need to consider for the gravitational energy capacity component. As mentioned earlier, each degree of freedom has an energy of $\frac{1}{2}RT$. It therefore has an energy capacity of $\frac{1}{2}R$. The gravitational energy capacity component is equal and opposite to this, i.e., $-\frac{1}{2}R$.

Therefore, C_T for an adiabatic process in a gravitational field,

$$C_T = \frac{1}{2}\alpha R + R - \frac{1}{2}R = \frac{1}{2}\alpha R + \frac{1}{2}R \tag{42}$$

$$\therefore \gamma = \frac{\frac{1}{2}\alpha R + \frac{1}{2}R}{\frac{1}{2}\alpha R} \tag{43}$$

$$= \frac{\alpha + 1}{\alpha} \tag{44}$$

Hence, for dry air in the light phase, the γ constant for an adiabatic process in a gravitational field is, $\gamma_g = \frac{6}{5} = 1.2$.

From Equation 34, we can now obtain a theoretical thermodynamic estimate for a for each of our γ values for dry air in the light phase:

- Isothermal process ($\gamma_i = 1$) $\Rightarrow a_i = \frac{1}{RT}$
- Adiabatic process with no field change ($\gamma_a = 1.4$) $\Rightarrow a_a = \frac{1}{1.4RT}$
- Adiabatic process in a gravitational field ($\gamma_g = 1.2$) $\Rightarrow a_g = \frac{1}{1.2RT}$

Other processes, such as phase changes, or the loss/gain of energy by radiation could alter the value of γ. Changes in the atmospheric composition can also change the γ values.

In determining how changes in the atmospheric composition affect γ, there are a number of factors which need to be considered:

1. Since γ is a function of the number of degrees of freedom, α, if the mean value of α increases or decreases as the atmospheric composition changes, then this will alter γ.

2. If a phase change releases or absorbs latent heat, or an exothermic/endothermic chemical reaction occurs, this may change C_T and/or C_V, and therefore could alter γ.

[4]Since PV=nRT, and n=1 for a mole, PV=RT, and therefore $\frac{d(PV)}{dT} = R$.

[5]Each vibrational mode has two degrees of freedom, one kinetic and one potential.

3. Similarly, if the atmospheric region absorbs or emits radiation (through some radiative process), this could also alter C_T and/or C_V.

4. Rearranging Equation 30, $\gamma = \frac{B}{P}$. Therefore, since B is defined in terms of changes in volume (dV), changes in volume brought about either directly by solid/liquid/gas transitions or indirectly by heat may change γ.

5. The effects of the gravitational field on the atmosphere need to be considered. From the derivation of γ_g, gravity clearly affects γ. Gravity can also indirectly affect γ, by changing the atmospheric composition, e.g., rain.

6. Electrostatic fields may also influence γ, particularly at higher altitudes, e.g., in the ionosphere.

7. Magnetic fields can affect γ in two ways - through the internal magnetic fields of the molecules or through interaction with the Earth's magnetic field.

Several atmospheric components need to be considered for describing the atmospheric barometric temperature profiles discussed in this paper:

- The N_2 and O_2 gases which comprise the bulk of the atmosphere.
- Water vapour (H_2O), which is particularly important in the boundary layer of the lower troposphere.
- Air that is in the "heavy phase".

We already calculated above theoretical values of γ for the dry N_2/O_2 gases for three thermodynamic processes. However, these values might have to be modified if the air is affected by one or other of the factors mentioned above, e.g., if the air gains or loses energy through latent heat, chemical reactions or radiation, or through changes in the Earth's magnetic field (since O_2 is paramagnetic).

If the water vapour concentration of the air changes, this has several different consequences, which can have different effects on γ at different points in the atmosphere. H_2O has a higher value of α, and so increasing the water content of air will typically increase the mean value of α of air (in the light phase), thereby reducing γ. But, the condensation of water vapour releases latent heat, while its evaporation requires latent heat, both of which can affect γ in opposite ways. So, rain events, for instance, may increase γ in one part of the atmosphere, but decrease γ in other parts.

In Paper II, we propose that the "heavy phase" of air involves the partial multimerization of oxygen (possibly involving nitrogen)[2]. However, regardless of its identity the phase change should have a number of effects on γ of the heavy phase air and its surroundings. For instance, the heavy phase may have a different value of α. In addition, phase changes tend to be isothermal while the latent ("hidden") heat is being absorbed/released. So, for regions where the phase change is on-going or incomplete, this should be an isothermal process, and we would expect $\gamma = \gamma_i$.

Like the condensation/evaporation of water vapour, the heavy phase/light phase transition should be accompanied by latent heat absorption/release. This should alter γ of the surrounding air. It may also involve the release (and possibly absorption) of radiation.

Finally, O_2 is paramagnetic, while some oxygen multimer species $(O_2)_n$ are diamagnetic. So, if the heavy phase includes diamagnetic oxygen multimers, this could change the magnetic properties of the air, and the interaction of the air with the Earth's magnetic field.

How to generate a theoretical barometric temperature profile

If we know the temperature, T_1 and pressure, P_1 at an initial location in the atmosphere (e.g., at ground level), and we know the γ values adopted by the air at different pressures for that air column, it is possible to theoretically derive the barometric temperature profile for that air column, within a given phase, using the following approach.

- Calculate the molar volume, $\overline{V_1}$, of the air at the initial location.

The molar volume, is defined as the mean volume occupied by 1 mole of the gas, i.e.,

$$\overline{V} = \frac{V}{n} \tag{45}$$

where n is the number of moles in the volume V. From the ideal gas law,

$$\overline{V_1} = \frac{V_1}{n_1} = \frac{RT_1}{P_1} \tag{46}$$

- Calculate the molar volume, $\overline{V_2}$, of the air at a second location, with a given pressure, P_2, close to the initial location.

From Equation 17,

$$dP = -B\frac{dV}{V} = -B\frac{d\overline{V}}{\overline{V}} \tag{47}$$

Since,

$$\frac{dV}{V} = \frac{d\overline{V}}{\overline{V}} \tag{48}$$

Combining Equations 30 and 47,

$$dP = -\gamma P\frac{d\overline{V}}{\overline{V}} \tag{49}$$

$$\therefore \frac{dP}{P} = -\gamma\frac{d\overline{V}}{\overline{V}} \tag{50}$$

Integrating both sides of the above equation between the corresponding limits $(P_1, \overline{V_1})$ and $(P_2, \overline{V_2})$,

$$\int_{P_1}^{P_2}\frac{dP}{P} = \int_{\overline{V_1}}^{\overline{V_2}} -\gamma\frac{d\overline{V}}{\overline{V}} \tag{51}$$

gives

$$\begin{aligned}\ln P_2 - \ln P_1 &= -\gamma\left(\ln\overline{V_2} - \ln\overline{V_1}\right) \\ &= \gamma\left(\ln\overline{V_1} - \ln\overline{V_2}\right)\end{aligned} \tag{52}$$

$$\therefore \ln\left(\frac{P_2}{P_1}\right) = \gamma\ln\left(\frac{\overline{V_1}}{\overline{V_2}}\right) \tag{53}$$

Exponentiating both sides gives,

$$\frac{P_2}{P_1} = \left(\frac{\overline{V_1}}{\overline{V_2}}\right)^{\gamma} \tag{54}$$

$$\therefore \left(\frac{P_2}{P_1}\right)^{\frac{1}{\gamma}} = \frac{\overline{V_1}}{\overline{V_2}} \tag{55}$$

$$\therefore \overline{V_2} = \overline{V_1} \div \left(\frac{P_2}{P_1}\right)^{\frac{1}{\gamma}} = \overline{V_1}\left(\frac{P_1}{P_2}\right)^{\frac{1}{\gamma}} \tag{56}$$

- Since we now know $\overline{V_2}$, and we are given P_2, we can calculate the temperature of the air at the second location, T_2 using the following relationship:

$$T_2 = \frac{P_2\overline{V_2}}{R} \tag{57}$$

- Repeat the above process to calculate T_{k+1} for P_{k+1} from (P_k, T_k) for all the given values of P being considered.

If, during a given step, γ changes, e.g., if a phase boundary is crossed, then the new γ value must used from then on instead.

References

[1] N.O.A.A., N.A.S.A., and U.S.A.F. *U.S. Standard Atmosphere 1976*. U.S. Government Printing Office. Washington, D.C., U.S., 1976, 227 pp. URL: http://ntrs.nasa.gov/archive/nasa/casi.ntrs.nasa.gov/19770009539_1977009539.pdf.

[2] M. Connolly and R. Connolly. "The physics of the Earth's atmosphere II. Multimerization of atmospheric gases above the troposphere". 22 (Atm. Sci.). Ver. 0.1 (non peer reviewed draft). 2014. URL: http://oprj.net/articles/atmospheric-science/22.

[3] M. Connolly and R. Connolly. "The physics of the Earth's atmosphere III. Pervective power". 25 (Atm. Sci.). Ver. 0.1 (non peer reviewed draft). 2014. URL: http://oprj.net/articles/atmospheric-science/25.

[4] A. W. Brewer. "Evidence for a world circulation provided by the measurements of helium and water vapour distribution in the stratosphere". *Quat. J. Roy. Meteor. Soc.* 75 (1949), pp. 351–363. DOI: 10.1002/qj.49707532603.

[5] A. Gettleman et al. "Radiation balance of the tropical tropopause layer". *J. Geophys. Res.* 109 (2004), p. D07103. DOI: 10.1029/2003JD004190.

[6] S. Fueglistaler et al. "Tropical tropopause layer". *Rev. Geophys.* 47 (2009), RG1004. DOI: 10.1029/2008RG000267.

[7] M. L. Salby and P. F. Callaghan. "Influence of the Brewer-Dobson circulation on stratosphere-troposphere exchange". *J. Geophys. Res.* 111 (2006), p. D21106. DOI: 10.1029/2006JD007051.

[8] W. J. M. Seviour, N. Butchart, and S. C. Hardiman. "The Brewer-Dobson circulation inferred from ERA-Interim". *Quat. J. Roy. Meteor. Soc.* 138 (2012), pp. 878–888. DOI: 10.1002/qj.966.

[9] P. N. Edwards. "History of climate modeling". *WIRES Clim. Change* 2 (2011), pp. 128–139. DOI: 10.1002/wcc.95.

[10] D. Brunt. "The transfer of heat by radiation and turbulence in the lower atmosphere". *Proc. R. Soc. London A* 124 (1929), pp. 201–218. DOI: 10.1098/rspa.1929.0108.

[11] R. T. Pierrehumbert. "Infrared radiation and planetary temperature". *Phys. Today* 64 (2011), pp. 33–38. DOI: 10.1063/1.3541943.

[12] S. B. Fels et al. "Infrared cooling rate calculations in operational general circulation models: Comparisons with benchmark computations". *J. Geophys. Res.* 96D (1991), pp. 9105–9120. DOI: 10.1029/91JD00516.

[13] J. Hansen et al. "Efficient three-dimensional global models for climate studies: Models I and II". *Mon. Weather Rev.* 111 (1983), pp. 609–662. DOI: 10.1175/1520-0493(1983)111<0609:ETDGMF>2.0.CO;2.

[14] G. A. Schmidt et al. "Present-day atmospheric simulations using GISS ModelE: Comparison to in situ, satellite, and reanalysis data". *J. Clim.* 19 (2006), pp. 153–192. DOI: 10.1175/JCLI3612.1.

[15] D. P. Lalas and F. Einaudi. "On the correct use of the wet adiabatic lapse rate in stability criteria of a saturated atmosphere". *J. Appl. Meteor.* 13 (1974), pp. 318–324. DOI: 10.1175/1520-0450(1974)013<0318:OTCUOT>2.0.CO;2.

[16] M.-D. Chou. "A solar radiation model for use in climate studies". *J. Atmos. Sci.* 49 (1992), pp. 762–772. DOI: 10.1175/1520-0469(1992)049<0762:ASRMFU>2.0.CO;2.

[17] S. Manabe and R. F. Strickler. "Thermal equilibrium of the atmosphere with a convective adjustment". *J. Atmos. Sci.* 21 (1964), pp. 361–385. DOI: 10.1175/1520-0469(1964)021<0361:TEOTAW>2.0.CO;2.

[18] T. G. Dopplick. "Radiative heating of the global atmosphere". *J. Atmos. Sci.* 29 (1972), pp. 1278–1294. DOI: 10.1175/1520-0469(1972)029<1278:RHOTGA>2.0.CO;2.

[19] A. A. Lacis and J. E. Hansen. "A parameterization for the absorption of solar radiation in the Earth's atmosphere". *J. Atmos. Sci.* 31 (1974), pp. 118–133. DOI: 10.1175/1520-0469(1974)031<0118:APFTAO>2.0.CO;2.

[20] G. N. Plass. "The carbon dioxide theory of climatic change". *Tellus* 8 (1956), pp. 140–154. DOI: 10.1111/j.2153-3490.1956.tb01206.x.

[21] J. T. Kiehl and K. E. Trenberth. "Earth's annual global mean energy budget". *Bull. Amer. Meteor. Soc.* 78 (1997), pp. 197–208. DOI: 10.1175/1520-0477(1997)078<0197:EAGMEB>2.0.CO;2.

[22] J. Tyndall. "The Bakerian Lecture: On the absorption and radiation of heat by gases and vapours, and on the physical connexion of radiation, absorption, and conduction". *Phil. Trans. Roy. Soc. London* 151 (1861), pp. 1–36. URL: http://www.jstor.org/stable/108724.

[23] Rayleigh and W. Ramsay. "Argon, a new constituent of the atmosphere". *Proc. Roy. Soc. London* 57 (1895), pp. 265–287. URL: http://www.jstor.org/stable/115394.

[24] M. Höpfner et al. "The natural greenhouse effect of atmospheric oxygen (O2) and nitrogen (N2)". *Geophys. Res. Lett.* 39 (2012), p. L10706. DOI: 10.1029/2012GL051409.

[25] M. F. Crawford, H. L. Welsh, and J. L. Locke. "Infra-red absorption of oxygen and nitrogen induced by intermolecular forces". *Phys. Rev.* 75 (1949), pp. 1607–1607. DOI: 10.1103/PhysRev.75.1607.

[26] S. Solomon et al. *Climate change 2007: The physical science basis. Contribution of Working Group 1 to the Third Assessment Report of the Intergovernmental Panel on Climate Change*. Cambridge University Press. Cambridge. New York., 2007, 1056pp. ISBN: 978-0521-70596-7. URL: http://www.ipcc.ch/.

[27] W. S. Broecker. "Climatic change: Are we on the brink of a pronounced global warming?" *Science* 189 (1975), pp. 460–463. DOI: 10.1126/science.189.4201.460.

[28] M. N. Berberan-Santos, E. N. Bodunov, and L. Pogliani. "On the barometric formula". *Am. J. Phys.* 65 (1996), pp. 404–412. DOI: 10.1119/1.18555.

[29] R. B. da Silveira et al. "WMO intercomparison of GPS radiosondes. Alcântara, Brazil, 20 May - 10 June 2001." Instruments and observing methods Report No. 90. WMO-TD No. 1314. World Meteorological Organization, Geneva, Switzerland. 2001. URL: http://www.wmo.int/pages/prog/www/IMOP/publications-IOM-series.html.

[30] J. Nash et al. "WMO intercomparison of high quality radiosonde systems. Vacoas, Mauritius, 2 - 25 February 2005. Final Report". World Meteorological Organization, Geneva, Switzerland. 2006. URL: http://www.wmo.int/pages/prog/www/IMOP/PastIntercomparisons.html.

[31] J. Nash et al. "WMO intercomparison of high quality radiosonde systems. Yangjiang, China, 12 July - 3 August 2010." Instruments and Observing Methods report No. 107. WMO-TD No. 1580. World Meteorological Organization, Geneva, Switzerland. 2011. URL: http://www.wmo.int/pages/prog/www/IMOP/publications-IOM-series.html.

[32] A. Arking et al. "ICRCCM Infrared (clear-sky) line-by-line radiative fluxes". *CDIAC* (1991). DOI: 10.3334/CDIAC/sar.db1002.

[33] R. G. Ellingson, J. Ellis, and S. B. Fels. "The intercomparison of radiation codes used in climate models: Long wave results". *J. Geophys. Res.* 96D (1991), pp. 8929–8953. DOI: 10.1029/90JD01450.

[34] A. Gore. *An inconvenient truth*. 1st. Rodale Books, 2006. ISBN: 978-1594865671.

[35] N. Stern. "The economics of climate change: The Stern review". In: Cambridge University Press. Cambridge. New York., 2007, 712pp. ISBN: 9780521700801.

[36] J. F. Kasting, D. P. Whitmire, and R. T. Reynolds. "Habitable zones around main sequence stars". *Icarus* 101 (1993), pp. 108–128. DOI: 10.1006/icar.1993.1010.

[37] H. Lammer et al. "What makes a planet habitable?" *Astron. Astro. Rev.* 17 (2009), pp. 181–249. DOI: 10.1007/s00159-009-0019-z.

[38] J. Schneider et al. "Defining and cataloging exoplanets: the exoplanet.eu database". *Astron. Astro.* 532 (2011), A79. DOI: 10.1051/0004-6361:201116713.

[39] J. D. Haigh. "The sun and the earth's climate". *Living Rev. Solar Phys.* 4 (2007), p. 2. URL: http://solarphysics.livingreviews.org/Articles/lrsp-2007-2/.

[40] J. Kirkby. "Cosmic rays and climate". *Surv. Geophys.* 28 (2007), pp. 333–375. DOI: 10.1007/s10712-008-9030-6.

[41] L. J. Gray et al. "Solar influences on climate". *Rev. Geophys.* 48 (2010), RG4001. DOI: 10.1029/2009RG000282.

[42] H. Svensmark. "Evidence of nearby supernovae affecting life on Earth". *Mon. Not. Roy. Astron. Soc.* 423 (2012), pp. 1234–1253. DOI: 10.1111/j.1365-2966.2012.20953.x.

[43] N. Scafetta and R. C. Willson. "ACRIM-gap and TSI trend issue resolved using a surface magnetic flux TSI proxy model". *Geophys. Res. Lett.* 36 (2009), p. L05701. DOI: 10.1029/2008GL036307.

[44] M. Lockwood and C. Fröhlich. "Recent oppositely directed trends in solar climate forcings and the global mean surface air temperature". *Proc. R. Soc. A* 463 (2007), pp. 2447–2460. DOI: 10.1098/rspa.2007.1880.

[45] G. Kopp and J. L. Lean. "A new, lower value of total solar irradiance: Evidence and climate significance". *Geophys. Res. Lett.* 38 (2011), p. L01706. DOI: 10.1029/2010GL045777.

[46] J. Lean. "Contribution of ultraviolet irradiance variations to changes in the Sun's total irradiance". *Science* 244 (1989), pp. 197–200. DOI: 10.1126/science.244.4901.197.

[47] J. D. Haigh. "The role of stratospheric ozone in modulating the solar radiative forcing of climate". *Nature* 370 (1994), pp. 544–546. DOI: 10.1038/370544a0.

[48] J. D. Haigh. "The impact of solar variability on climate". *Science* 272 (1996), pp. 981–984. DOI: 10.1126/science.272.5264.981.

[49] D. Shindell et al. "Solar cycle variability, ozone and climate". *Science* 284 (1999), pp. 305–308. DOI: 10.1126/science.284.5412.305.

[50] M. Salby and P. Callaghan. "Connection between the solar cycle and the QBO: The missing link". *J. Clim.* 13 (2000), pp. 2652–2662. DOI: 10.1175/1520-0442(1999)012<2652:CBTSCA>2.0.CO;2.

[51] K. Labitzke and H. Van Loon. "Connection between the troposphere and stratosphere on a decadal scale". *Tellus* 47A (1995), pp. 275–286. DOI: 10.1034/j.1600-0870.1995.t01-1-00008.x.

[52] K. Labitzke. "Solar variation and stratospheric response". *Space Sci. Rev.* 125 (2006), pp. 247–2601. DOI: 10.1007/s11214-006-9061-6.

[53] M. Salby and P. Callaghan. "Evidence of the solar cycle in the general circulation of the stratosphere". *J. Clim.* 17 (2004), pp. 34–46. DOI: 10.1175/1520-0442(2004)017<0034:EOTSCI>2.0.CO;2.

[54] M. L. Salby and P. F. Callaghan. "Relationship of the quasi-biennial oscillation to the stratospheric signature of the solar cycle". *J. Geophys. Res.* 111 (2006), p. D06110. DOI: 10.1029/2005JD006012.

[55] K. Kodera and Y. Kuroda. "Dynamical response to the solar cycle". *J. Geophys. Res.* 107D (2002), p. 4749. DOI: 10.1029/2002JD002224.

[56] L. L. Hood. "Thermal response of the tropical tropopause region to solar ultraviolet variations". *Geophys. Res. Lett.* 30 (2003), p. 2215. DOI: 10.1029/2003GL018364.

[57] M. P. Baldwin and T. J. Dunkerton. "The solar cycle and stratosphere-troposphere dynamical coupling". *J. Atm. Sol.-Terr. Phys.* 67 (2005), pp. 71–82. DOI: 10.1016/j.jastp.2004.07.018.

[58] A. Hannachi, T. Woollings, and K. Fraedrich. "The North Atlantic jet stream: a look at preferred positions, paths and transitions". *Quat. J. Roy. Meteor. Soc.* 138 (2012), pp. 862–877. DOI: 10.1002/qj.959.

[59] J. Vial and T. J. Osborn. "Assessment of atmospheric-ocean general circulation model simulations of winter northern hemisphere atmospheric blocking". *Clim. Dyn.* 39 (2012), pp. 95–112. DOI: 10.1007/s00382-011-1177-z.

[60] T. Woollings and M. Blackburn. "The North Atlantic jet stream under climate change and its relation to the NAO and EA patterns". *J. Clim.* 25 (2012), pp. 886–902. DOI: 10.1175/JCLI-D-11-00087.1.

[61] S. Häkkinen, P. B. Rhines, and D. L. Worthen. "Atmospheric blocking and Atlantic multidecadal ocean variability". *Science* 334 (2011), pp. 655–659. DOI: 10.1126/science.1205683.

[62] R. D. Hudson. "Measurements of the movement of the jet streams at mid-latitudes, in the northern and southern hemi-

spheres, 1979 to 2010". *Atmos. Chem. Phys.* 12 (2012), pp. 7797–2012. DOI: 10.5194/acp-12-7797-2012.

[63] H. van Loon and J. C. Rogers. "The seesaw in winter temperatures between Greenland and northern Europe. Part I: General description". *Mon. Wea. Rev.* 106 (1978), pp. 296–310. DOI: 10.1175/1520-0493(1978)106<0296:TSIWTB>2.0.CO;2.

[64] K. Guirguis et al. "Recent warm and cold daily winter temperature extremes in the Northern Hemisphere". *Geophys. Res. Lett.* 38 (2011), p. L17701. DOI: 10.1029/2011GL048762.

[65] G. Ouzeau et al. "European cold winter 2009-2010: How unusual in the instrumental record and how reproducible in the ARPEGE-Climat model?" *Geophys. Res. Lett.* 38 (2011), p. L11706. DOI: 10.1029/2011GL047667.

[66] J. Cohen et al. "Winter 2009-2010: A case study of an extreme Arctic Oscillation event". *Geophys. Res. Lett.* 37 (2010), p. L17707. DOI: 10.1029/2010GL044256.

[67] J. Cattiaux et al. "Winter 2010 in Europe: A cold extreme in a warming climate". *Geophys. Res. Lett.* 37 (2010), p. L20704. DOI: 10.1029/2010GL044613.

[68] J. Liu et al. "Impact of declining Arctic sea ice on winter snowfall". *Proc. Nat. Acad. Sci.* 109 (2012), pp. 4074–4079. DOI: 10.1073/pnas.1114910109.

[69] M. Lockwood et al. "Are cold winters in Europe associated with low solar activity?" *Environ. Res. Lett.* 5 (2010), p. 024001. DOI: 10.1088/1748-9326/6/2/024001.

[70] F. Sirocko, H. Brunck, and S. Pfahl. "Solar influence on winter severity in central Europe". *Geophys. Res. Lett.* 39 (2012), p. L16704. DOI: 10.1029/2012GL052412.

[71] G. H. Roe and R. S. Lindzen. "The mutual interaction between continental-scale ice sheets and atmospheric stationary waves". *J. Clim.* 14 (2001), pp. 1450–1465. DOI: 10.1175/1520-0442(2001)014<1450:TMIBCS>2.0.CO;2.

[72] G. H. Roe and R. S. Lindzen. "A one-dimensional model for the interaction between continental-scale ice sheets and atmospheric stationary waves". *Clim. Dyn.* 17 (2001), pp. 479–487. DOI: 10.1007/s003820000123.

[73] C. Jackson. "Sensitivity of stationary wave amplitude to regional changes in Laurentide ice sheet topography in single-layer models of the atmosphere". *J. Geophys. Res.* 105D (2000), pp. 24443–24454. DOI: 10.1029/2000JD900377.

[74] C. Wunsch. "Abrupt climate change: An alternative view". *Quat. Res.* 65 (2006), pp. 191–203. DOI: 10.1016/j.yqres.2005.10.006.

[75] V. Courtillot et al. "Are there connections between the Earth's magnetic field and climate?" *Earth Planet. Sci. Lett.* 253 (2007), pp. 328–339. DOI: 10.1016/j.epsl.2006.10.032.

[76] N. Scafetta. "A shared frequency set between the historical mid-latitude aurora records and the global surface temperature". *J. Atm. Sol.-Terr. Phys.* 74 (2012), pp. 145–163. DOI: 10.1016/j.jastp.2011.10.013.

[77] G. L. Siscoe. "Evidence in the auroral record for secular solar variability". *Rev. Geophys. Space Phys.* 18 (1980), pp. 647–658. DOI: 10.1029/RG018i003p00647.

[78] J. Bochníček and P. Hejda. "The winter NAO pattern changes in association with solar and geomagnetic activity". *J. Atm. Sol.-Terr. Phys.* 67 (2005), pp. 17–32. DOI: 10.1016/j.jastp.2004.07.014.

[79] R. F. Keeling and S. R. Shertz. "Seasonal and interannual variations in atmospheric oxygen and implications for the global carbon cycle". *Nature* 358 (1992), pp. 723–727. DOI: 10.1038/358723a0.

[80] C. Sirignano et al. "Atmospheric oxygen and carbon dioxide observations from two European coastal stations 2000-2005: continental influence, trend changes and APO climatology". *Atmos. Chem. Phys.* 10 (2010), pp. 1599–1615. DOI: 10.5194/acp-10-1599-2010.

[81] J. D. Neelin. *Climate change and climate modeling.* 1st. Cambridge University Press, 2011. ISBN: 978-0521602433.